© 2020. Published by The Company of Biologists Ltd | Journal of Cell Science (2021) 134, jcs246421. doi:10.1242/jcs.246421

RESEARCH ARTICLE

SPECIAL ISSUE: CELL BIOLOGY OF HOST–PATHOGEN INTERACTIONS

Protein tyrosine phosphatase 1B is involved in efficient type I interferon secretion upon viral infection

Elisa Reimer[1,‡], Markus Stempel[1,2,‡], Baca Chan[1,*], Hanna Bley[1] and Melanie M. Brinkmann[1,2,§]

ABSTRACT

Protein tyrosine phosphatase 1B (PTP1B, also known as PTPN1) is a negative regulator of the leptin and insulin signalling pathways. This phosphatase is of great interest as PTP1B-knockout mice are protected against the development of obesity and diabetes. Here, we provide evidence for a novel function of PTP1B that is independent of its phosphatase activity, but requires its localisation to the membrane of the endoplasmic reticulum. Upon activation of pattern recognition receptors, macrophages and plasmacytoid dendritic cells from PTP1B-knockout mice secrete lower amounts of type I interferon (IFN) than cells from wild-type mice. In contrast, secretion of the proinflammatory cytokines TNFα and IL6 was unaltered. While PTP1B deficiency did not affect *Ifnb1* transcription, type I IFN accumulated in macrophages, suggesting a role for PTP1B in mediating secretion of type I IFN. In summary, we have uncovered that PTP1B positively regulates the type I IFN response by promoting secretion of key antiviral cytokines.

KEY WORDS: Herpesvirus, Innate immunity, TLR, cGAS, STING, RIG-I, UNC93B, Type I IFN, Cytomegalovirus, Cytokine secretion, Pattern recognition receptor

INTRODUCTION

Early detection of invading pathogens is of vital importance to host survival. For this purpose, cells possess a variety of germline-encoded pattern recognition receptors (PRRs), including Toll-like receptors (TLRs), which localise on the cell surface or within endosomal compartments, as well as intracellular RNA and DNA sensors. PRRs not only sense conserved microbial structures but also aberrantly localised nucleic acids of infected cells, and subsequently induce a fast and efficient immune response leading to the expression of proinflammatory cytokines and type I interferons (IFNs) (Paludan and Bowie, 2013; Iwasaki, 2012; Goubau et al., 2013). Type I IFNs were first identified in 1957 by Isaacs and Lindenmann (1957), with follow up studies showing that these cytokines are rapidly induced upon viral infection thereby serving as major effectors for the execution and regulation of the innate immune response (Stark et al., 1998; Pestka, 2007; Content, 2009). Following secretion, type I IFNs bind to cell surface IFNα/β-receptor (IFNAR, also known as IFNAR1) in a paracrine and autocrine manner leading to the induction of IFNAR signalling. Activation of the IFNAR upon ligand binding results in the activation of associated intracellular tyrosine kinase 2 (Tyk2) and Janus kinase 1 (Jak1) proteins, which then activate the transcription factors signal transducer and activator of transcription 1 (STAT1) and STAT2 (Stark and Darnell, 2012), subsequently inducing the transcription of interferon-stimulated genes (ISGs). Over the past two decades, the identification of different classes of PRRs and the characterisation of the respective downstream signalling pathways have expanded our knowledge regarding innate immune activation and the response to infection (Mogensen, 2009; Wu and Chen, 2014). While the mechanisms leading to induction of cytokine expression and their antiviral effector functions have been described in great detail, astonishingly little is known about intracellular trafficking and release of cytokines from cells. The trafficking pathway and molecular machinery for some proinflammatory cytokines, i.e. interleukin 6 (IL6), tumor necrosis factor α (TNFα, also known as TNF) and IL10, has been comprehensively studied (Manderson et al., 2007; Murray et al., 2005a,b; Murray and Stow, 2014). However, despite their central and prominent antiviral role, the mechanisms of type I IFN trafficking and release remain poorly understood.

The protein tyrosine phosphatase 1B (PTP1B, also known as PTPN1) has been the focus of extensive studies owing to its involvement in several important cellular pathways. PTP1B is a classical non-receptor tyrosine phosphatase (Feldhammer et al., 2013). While it does not have a transmembrane domain, PTP1B has a 35-residue C-terminal tail that anchors the protein to the ER membrane facing the cytoplasm (Frangioni et al., 1992; Woodford-Thomas et al., 1992). The N-terminus contains the PTP domain with the cysteine residue at position 215 necessary for its catalytic activity (Jia et al., 1995). Moreover, since the interactions of phosphatases with their substrates are transient and difficult to detect, a substrate-trapping mutant of PTP1B (D181A) that shows strongly diminished phosphatase activity has been developed to identify new substrates of PTP1B (Flint et al., 1997; Blanchetot et al., 2005).

PTP1B is the main enzyme involved in insulin receptor desensitisation and acts by dephosphorylating the insulin receptor as well as insulin receptor substrate-1 (Chernoff, 1999; Seely et al., 1996; Elchebly et al., 1999; Klaman et al., 2000; Goldstein et al., 2000). Since PTP1B also plays an important role in obesity control, it is a very attractive drug target (Zhang and Zhang, 2007). It dephosphorylates the effector kinase Jak2, thus attenuating the leptin signalling pathway, which is crucial for energy regulation in the host (Zabolotny et al., 2002; Kaszubska et al., 2002). Moreover, the epidermal growth factor receptor (EGFR) has also been shown to be a substrate of PTP1B. After its activation and internalisation, EGFR is dephosphorylated by PTP1B, and PTP1B was shown to be

[1]Helmholtz Centre for Infection Research, Viral Immune Modulation Research Group, Inhoffenstr. 7, 38124 Braunschweig, Germany. [2]Technische Universität Braunschweig, Institute of Genetics, Spielmannstr. 7, 38106 Braunschweig, Germany.
*Present address: Viral Genomics Group, Institute for Respiratory Health, University of Western Australia, Nedlands, Australia.
‡These authors contributed equally to this work

§Author for correspondence (m.brinkmann@tu-bs.de)

M.S., 0000-0002-9240-3987; B.C., 0000-0003-0788-9503; M.M.B., 0000-0001-5431-6527

Handling Editor: Michael Way
Received 13 March 2020; Accepted 19 March 2020

Journal of Cell Science (2021) 134, jcs246421. doi:10.1242/jcs.246421

critically involved in the trafficking of EGFR to endosomes and multivesicular bodies (Flint et al., 1997; Eden et al., 2010; Sangwan et al., 2011; Stuible et al., 2010). A recent study connected PTP1B with HSV-1 infection and showed that PTP1B is required for efficient cell-to-cell spread of HSV-1 in a phosphatase-activity dependent manner (Carmichael et al., 2018). Since Jak2, Tyk2 and STAT6 have been shown to be substrates of PTP1B, some studies have described a role for PTP1B in innate immune signalling. By using an overexpression and siRNA approach, one study reported that PTP1B negatively regulates TLR-dependent proinflammatory cytokine and type I IFN production in RAW264.7 macrophages in a manner that was dependent on its phosphatase activity (Xu et al., 2008). Another study showed that the microRNA miR-744 targets PTP1B in human renal mesangial cells, resulting in enhanced expression of ISGs upon IFNAR activation (Zhang et al., 2015). Través and colleagues analysed the role of PTP1B in human and murine macrophages after stimulation with proinflammatory and inflammatory stimuli and saw enhanced responses in the absence of PTP1B *in vitro* and *in vivo* (Través et al., 2014). More recently, PTP1B and the closely related class I nonreceptor protein tyrosine phosphatase TC-PTP (also known as PTPN2) have been associated with STING-mediated signalling. However, the observed phenotype of attenuated antiviral responses through dephosphorylation and subsequent proteasomal degradation of STING was mostly attributed to TC-PTP rather than PTP1B, and could not be verified *in vivo* (Xia et al., 2019). Notably, all these studies reported that the phosphatase activity of PTP1B was important for the observed phenotypes.

Here, we identify a novel function of PTP1B that is independent of its phosphatase activity, but requires localisation of PTP1B to the membrane of the endoplasmic reticulum (ER). We show that PTP1B positively regulates the secretion of type I IFNs upon signalling of the PRRs cGAS, RIG-I (also known as DDX58), TLR7 and TLR9 *in vitro* in different innate immune cells and *in vivo*, but neither the transcription nor translation of type I IFNs . Notably, secretion of the proinflammatory cytokines TNFα and IL6 is not affected by the absence of PTP1B.

Taken together, our results show that PTP1B specifically promotes the secretion of type I IFNs independently of its phosphatase activity, and therewith have revealed a novel feature of PTP1B in the context of the PRR-mediated innate immune response to viral infection.

RESULTS

The type I IFN response downstream of endosomal TLRs is reduced in the absence of PTP1B, while the proinflammatory cytokine response is intact

We originally identified PTP1B in an affinity purification coupled to mass spectrometry approach as an interaction partner of the TLR chaperone UNC93B (also known as UNC93B1). The membrane protein UNC93B tightly binds to endosomal TLRs and is essential for their proper trafficking from the ER to endosomes, from where these TLRs initiate their signalling cascade following pathogen sensing (Tabeta et al., 2006; Brinkmann et al., 2007). UNC93B carrying the point mutation H412R cannot bind to TLRs and therefore, the TLRs cannot traffic to induce proinflammatory cytokine and type I IFN production from endosomes (Tabeta et al., 2006; Brinkmann et al., 2007). Based on the localisation of PTP1B to the cytoplasmic face of the ER and its prominent role in the trafficking of the EGFR (Flint et al., 1997; Eden et al., 2010; Sangwan et al., 2011; Stuible et al., 2010), we hypothesised that it could be involved in the control of trafficking of the UNC93B–TLR complex from the ER to the endosomal compartment. To assess whether PTP1B is involved in innate immune signalling, we first sought to analyse secretion of the cytokines IFNα and TNFα upon TLR7 and TLR9 stimulation, which occurs in an UNC93B-dependent manner. Given that TLR activation induces barely detectable levels of type I IFNs in bone marrow-derived macrophages (BMDMs), we used freshly isolated bone marrow cells that contain plasmacytoid dendritic cells (pDCs), which are known to secrete high levels of type I IFNs upon TLR7 or TLR9 stimulation.

We observed that bone marrow cells from PTP1B-knockout ($PTP1B^{-/-}$) mice secrete less IFNα than those from wild-type (WT) mice after stimulation with CpG DNA, a TLR9 ligand (Fig. 1A), or poly(U), a TLR7 ligand (Fig. 1B). In contrast, the TNFα and IL6 responses were equal between WT and $PTP1B^{-/-}$ cells (Fig. 1A,B; Fig. S1A). As expected, TLR7- and TLR9-dependent IFNα, TNFα and IL6 responses were completely abrogated in cells of 3d mice carrying the point mutation H412R in UNC93B (Tabeta et al., 2006; Brinkmann et al., 2007), as was the TLR9-mediated response to CpG DNA in $TLR9^{-/-}$ bone marrow cells (Fig. 1A,B; Fig. S1A). Next, we used a natural stimulus of TLR9, and infected bone marrow cells from WT and $PTP1B^{-/-}$ mice with murine cytomegalovirus (MCMV) (Tabeta et al., 2006, 2004; Bussey et al., 2019). As expected, type I IFNs and proinflammatory cytokine responses were abolished in $TLR9^{-/-}$ and 3d cells following MCMV infection, while they were reduced or unaltered, respectively, in $PTP1B^{-/-}$ cells (Fig. 1C; Fig. S1A).

Since cells from $PTP1B^{-/-}$ mice do not recapitulate the phenotype seen in cells from UNC93B-deficient mice, we conclude that PTP1B is not involved in the trafficking of the UNC93B–TLR complex from the ER to the endosomal compartment. Importantly, however, our results show that PTP1B plays a role in innate immunity, as it is necessary for a competent type I IFN response in bone marrow cells upon TLR stimulation.

The type I IFN response downstream of the pattern recognition receptors cGAS and RIG-I is diminished in PTP1B-deficient BMDMs

Next, we assessed whether PTP1B acts specifically on the type I IFN response mediated by TLRs or whether it also affects signalling downstream of the PRRs cGAS and RIG-I. Since macrophages secrete substantial amounts of type I IFNs and TNFα upon stimulation of the DNA-sensing PRR cGAS and the RNA-sensing PRR RIG-I, we stimulated primary MCSF-differentiated BMDMs isolated from WT, $PTP1B^{-/-}$ or $STING^{-/-}$ mice with the synthetic cGAS ligand IFN-stimulatory DNA (ISD) (Fig. 2A), the cGAS enzymatic product and STING ligand cGAMP (Fig. 2B), or through infection with MCMV (Fig. 2C). We observed that the cGAS–STING-dependent type I IFN response was diminished in the absence of PTP1B. As expected, $STING^{-/-}$ BMDMs, which are deficient in cytosolic DNA sensing, did not respond to these stimuli (Fig. 2A–C).

Next, we stimulated WT, $PTP1B^{-/-}$ or $MAVS^{-/-}$ BMDMs with the synthetic RIG-I ligand 5′ triphosphorylated double stranded RNA (5′ppp-dsRNA) (Fig. 2D) or through infection with the RNA virus Newcastle disease virus (NDV) (Fig. 2E), which is efficiently sensed by RIG-I in this cell type. For both RIG-I stimuli, we observed the same phenotype as for the cGAS pathway – the type I IFN response in $PTP1B^{-/-}$ BMDM was reduced compared to that in WT BMDMs (Fig. 2D,E). As expected, the type I IFN response was completely absent in BMDM lacking the RIG-I adaptor protein MAVS (Fig. 2D,E).

Strikingly, the TNFα response remained unaltered upon stimulation of the cGAS–STING or RIG-I–MAVS pathway in the absence of

Journal of Cell Science (2021) 134, jcs246421. doi:10.1242/jcs.246421

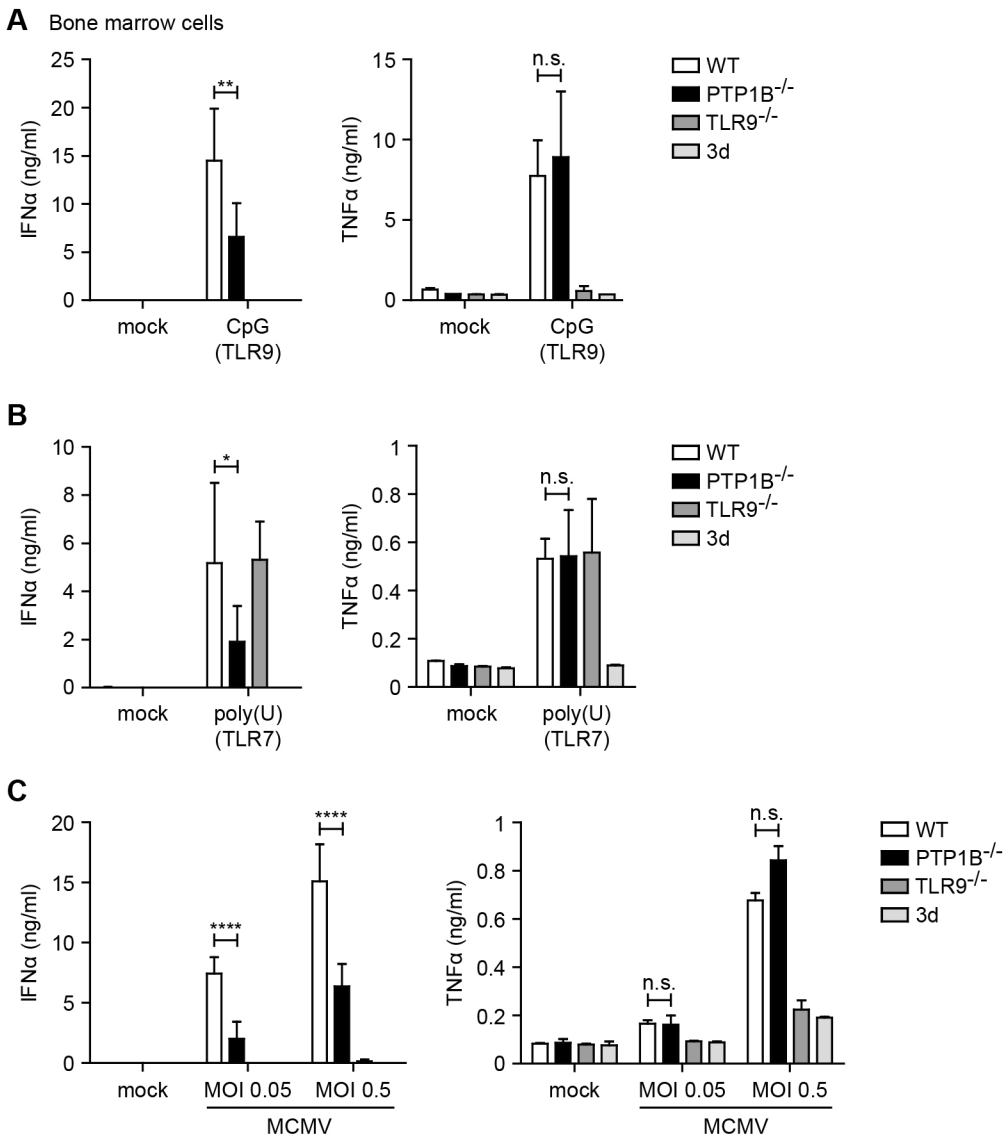

Fig. 1. Type I IFN production in bone marrow cells is reduced in the absence of PTP1B, while TNFα levels are unaffected. (A–C) Bone marrow cells isolated from WT, PTP1B$^{-/-}$, TLR9$^{-/-}$ or 3d (deficient in endosomal TLR signalling) mice were stimulated with 1 µM of the TLR9 ligand CpG 2336 (A), transfected with 1 µg/ml of the TLR7 ligand poly(U) (B) or infected with murine cytomegalovirus (MCMV) at the indicated MOI (C) for 22 h. Levels of IFNα (left panels) and TNFα (right panels) in supernatants were determined by ELISA. Mock samples were treated with medium only. Results are shown as mean±s.d. of five (IFNα) or two (TNFα) independent experiments with biological duplicates. *P<0.05; **P<0.01; ****P<0.0001; n.s., not significant (unpaired two-tailed Student's t-test).

PTP1B (Fig. 2F), consistent with our observations following TLR stimulation. In line with these results, levels of secreted IL6 upon cGAMP stimulation or MCMV infection were unaffected in PTP1B$^{-/-}$ BMDMs compared to those seen in WT BMDMs (Fig. S1B). To ensure that the reduced type I IFN response observed in bone marrow cells and BMDMs from PTP1B$^{-/-}$ mice was not due to lower numbers of pDCs in the bone marrow or differences in BMDM differentiation, respectively, we characterised these cell types by flow cytometry using the respective markers, and did not detect any differences when compared to cells from WT mice (Fig. S1C,D).

These results suggest that PTP1B contributes to an efficient type I IFN response downstream of the PRRs cGAS, RIG-I and TLR, while it plays no role in the TNFα response mediated by these PRRs.

PTP1B does not affect PRR-mediated type I IFN transcription or signalling downstream of the IFNAR

Next, we systematically analysed the incremental steps of the PRR-mediated type I IFN response in PTP1B$^{-/-}$ BMDMs. Multiple scenarios are possible, such as a role for PTP1B in the signalling cascade downstream of PRRs, which would affect type I IFN transcription. Alternatively, PTP1B may be involved in signalling downstream of the type I IFN receptor (IFNAR) since PTP1B was previously shown to act on JAK-STAT-mediated signalling events (Myers et al., 2001; Lu et al., 2008) and since IFNAR signalling provides a positive feedback loop for type I IFN expression.

To test these two possibilities, we first stimulated the cGAS–STING pathway in WT and PTP1B$^{-/-}$ BMDMs with the cGAS ligand ISD or through MCMV infection, and analysed activation by immunoblotting for the phosphorylated (activated) versions of the kinase TANK-binding kinase 1 (TBK1) and the transcription factor IFN-regulatory factor 3 (IRF3), which both act downstream of cGAS-mediated DNA sensing. As shown in Fig. 3A and quantified in Fig. S2A, we detected no differences in the activation levels of these crucial players of the cGAS–STING signalling pathway between WT and PTP1B-deficient BMDMs.

Next, we analysed the induction of type I IFN transcription downstream of cGAS–STING (Fig. 3B–D) and RIG-I–MAVS (Fig. 3D) signalling by quantitative RT-PCR (qPCR). We did not detect any differences between WT and PTP1B$^{-/-}$ BMDMs, while, as expected, type I IFN transcription was not detected in STING$^{-/-}$ BMDMs upon MCMV infection or stimulation with cGAMP or ISD (Fig. 3B–D). In addition, we analysed the induction of type I IFN transcription *ex vivo* in BMDM from IFNβ reporter mice

Journal of Cell Science (2021) 134, jcs246421. doi:10.1242/jcs.246421

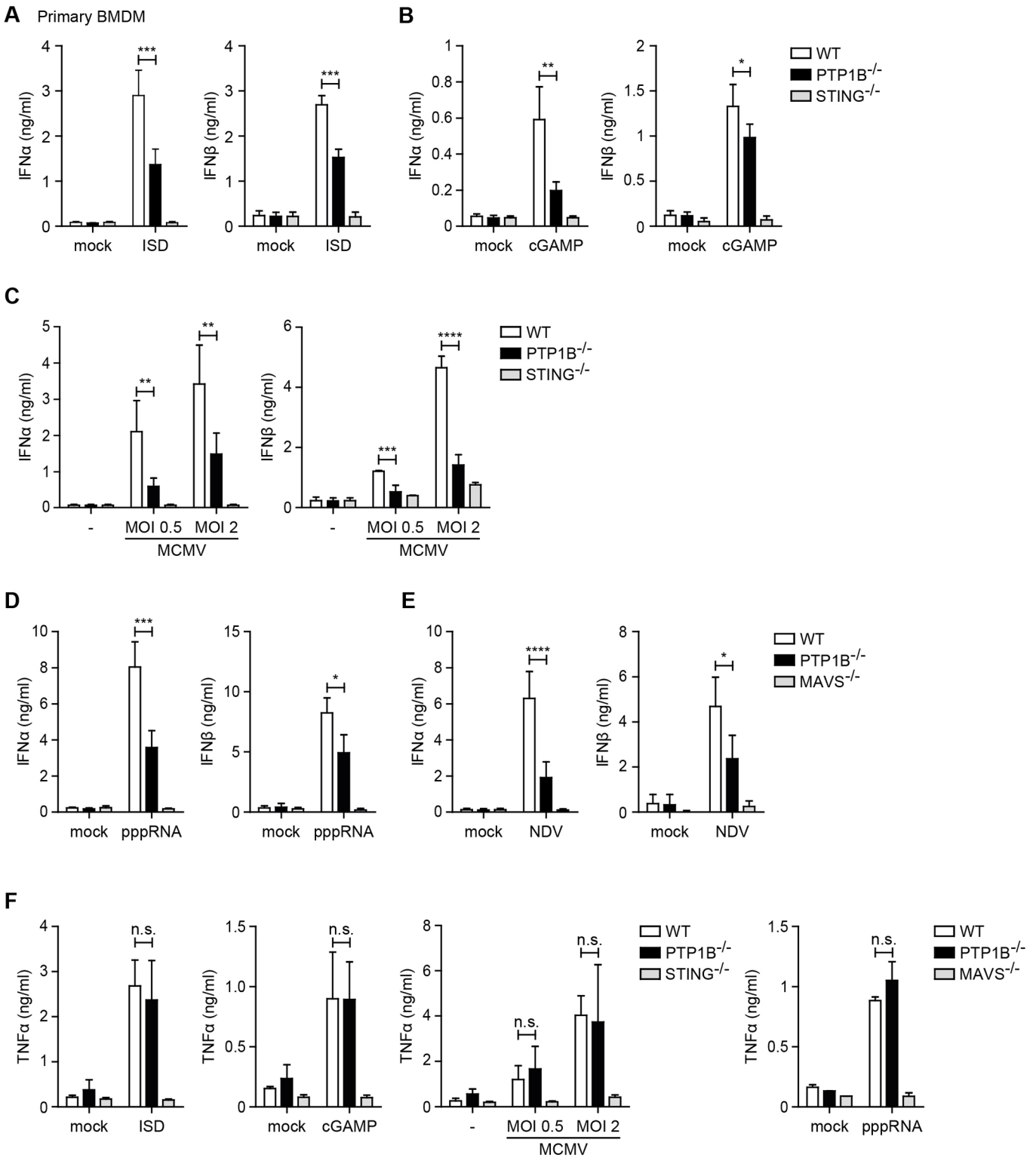

Fig. 2. PTP1B is required for cGAS- and RIG-I-mediated type I IFN responses in BMDMs, but dispensable for their TNFα response. (A–E) Primary MCSF-differentiated BMDMs prepared from WT, PTP1B$^{-/-}$ and STING$^{-/-}$ (A–C), or WT, PTP1B$^{-/-}$ and MAVS$^{-/-}$ (D,E) mice were transfected with 3 µg/ml IFN-stimulatory DNA (ISD) (A), 3 µg/ml cGAMP (B), infected with MCMV (C), transfected with 3 µg/ml 5′ppp-dsRNA (pppRNA) (D) or infected with Newcastle disease virus (NDV) (E). At 16 h post stimulation or infection, levels of IFNα and IFNβ in supernatants were determined by ELISA. (F) Primary BMDMs prepared from WT, PTP1B$^{-/-}$, STING$^{-/-}$ and MAVS$^{-/-}$ mice were transfected with 1 µg/ml ISD, 3 µg/ml cGAMP, infected with MCMV or transfected with 3 µg/ml 5′ppp-dsRNA. At 16 h post stimulation or infection, levels of TNFα in supernatants were determined by ELISA. Mock samples were treated with Lipofectamine only (transfection reagent), '-' samples were treated with medium only. Results are shown as mean±s.d. of three (IFNα) or two (IFNβ, TNFα) combined independent experiments performed with biological duplicates. Four independent experiments for IFNα and TNFα and two independent experiments for IFNβ were performed. *P<0.05; **P<0.01; ***P<0.001; ****P<0.0001; n.s., not significant (unpaired two-tailed Student's t-test).

Journal of Cell Science (2021) 134, jcs246421. doi:10.1242/jcs.246421

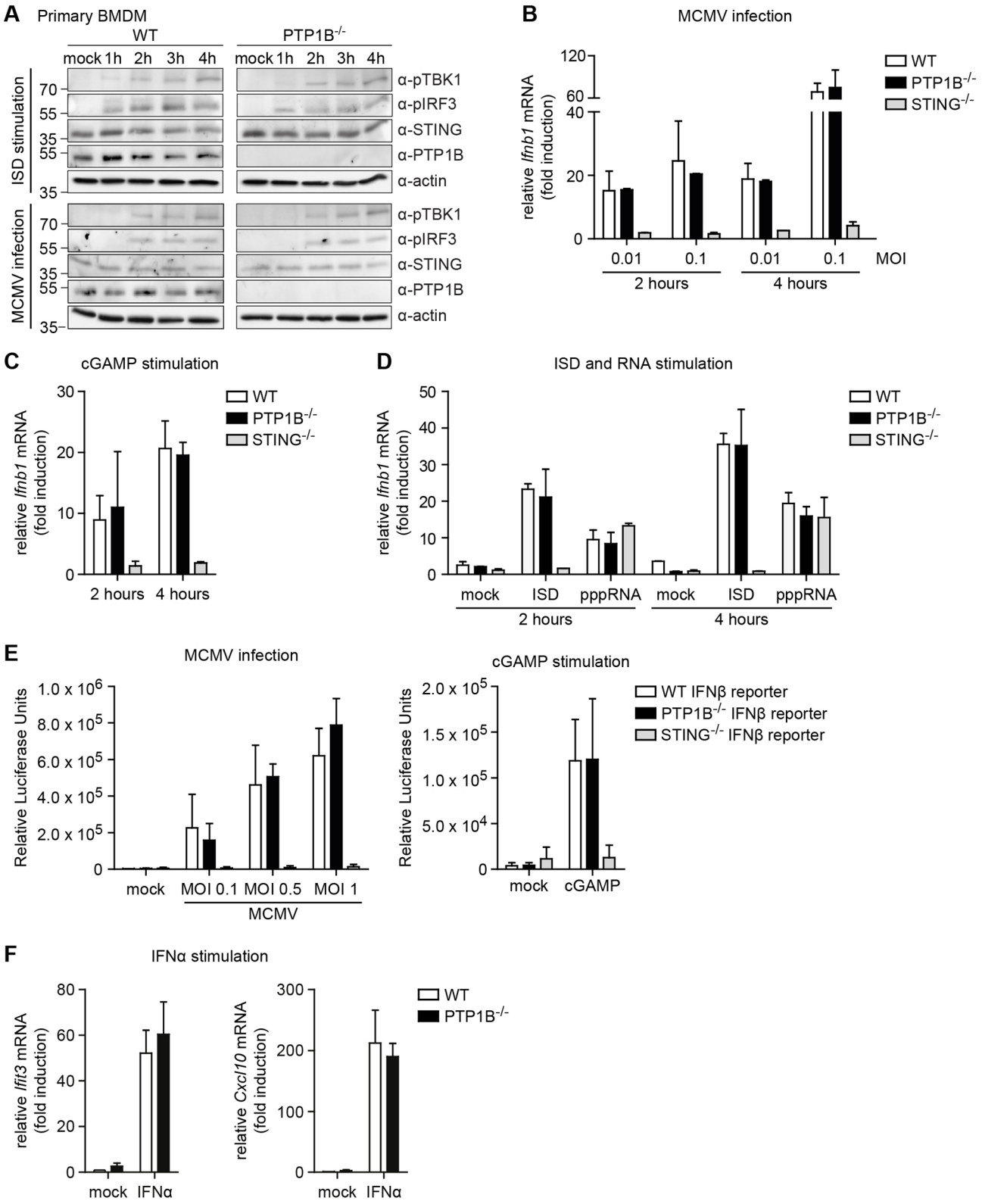

Fig. 3. See next page for legend.

(Lienenklaus et al., 2009). In this conditional mouse line, the IFNβ (*Ifnb1*) sequence is replaced by the sequence encoding reporter firefly luciferase. For this study, we used mice that were heterozygous for the targeted mutation ($IFN\beta^{+/\Delta\beta\text{-luc}}$), which allows IFNβ production from the functional WT allele. We crossed these heterozygous IFNβ reporter mice (herein referred to as WT IFNβ reporter) with $PTP1B^{-/-}$ or $STING^{-/-}$ mice to obtain $PTP1B^{-/-}/IFN\beta^{+/\Delta\beta\text{-luc}}$ ($PTP1B^{-/-}$ IFNβ reporter) and $STING^{-/-}/IFN\beta^{+/\Delta\beta\text{-luc}}$ ($STING^{-/-}$ IFNβ reporter) mice, respectively. We differentiated bone marrow extracted from these reporter mice with MCSF to obtain

Journal of Cell Science (2021) 134, jcs246421. doi:10.1242/jcs.246421

Fig. 3. PTP1B is not involved in PRR-mediated transcription of type I IFNs or signalling downstream of IFNAR. (A) BMDMs generated from WT or PTP1B$^{-/-}$ mice were left untreated (mock), stimulated with ISD (upper panel) or infected with MCMV (MOI 0.5, lower panel) for 1, 2, 3 or 4 h. Cells were lysed and protein levels of phosphorylated TBK1 (pTBK1), phosphorylated IRF3 (pIRF3), STING, PTP1B and actin were detected by immunoblotting with the respective antibodies. One representative experiment out of two independent experiments is shown. (B–D) BMDMs generated from WT, PTP1B$^{-/-}$ or STING$^{-/-}$ mice were left untreated or infected with MCMV at an MOI of 0.01 or 0.1 (B), stimulated by addition of 10 µg/ml cGAMP (C), or transfected with 3 µg/ml ISD or 1 µg/ml 5′ppp-dsRNA (pppRNA) (D). At 2 and 4 h post infection or stimulation, total RNA was extracted to determine *Ifnb1* mRNA transcript levels by qRT-PCR. Results are shown as mean±s.d. for one out of two independent experiments performed in biological duplicates. (E) BMDMs from WT IFNβ reporter, PTP1B$^{-/-}$ IFNβ reporter or STING$^{-/-}$ IFNβ reporter mice were infected with MCMV at MOI 0.1, 0.5 and 1 (left panel) or transfected with 3 µg/ml cGAMP (right panel). At 3 h after stimulation, cells were lysed for analysis of luciferase activity, which measures IFNβ transcription. Results are shown as mean±s.d. of two independent experiments performed with biological duplicates. (F) BMDMs generated from WT and PTP1B$^{-/-}$ mice were left unstimulated or were stimulated with 100 U/ml IFNα for 4 h and expression of the ISGs *Ifit3* (left panel) and *Cxcl10* (right panel) was analysed by qRT-PCR. Results are shown as mean±s.d. of two independent experiments performed with biological duplicates. Data in B–D and F were normalised to the level of the housekeeping gene *Rpl8* and fold induction was calculated relative to unstimulated WT cells. Differences between datasets were not significant if not stated otherwise.

BMDMs, stimulated them by MCMV infection or with cGAMP addition, and measured luciferase activity. Consistent with our qPCR results in PTP1B$^{-/-}$ BMDM (Fig. 3B–D), *Ifnb1* transcription was equal between BMDM from WT and PTP1B$^{-/-}$ IFNβ reporter mice, while, as expected, no response was detected from cells derived from STING$^{-/-}$ IFNβ reporter mice (Fig. 3E).

To determine a potential impact of PTP1B on the IFNAR signalling cascade, we stimulated WT and PTP1B$^{-/-}$ BMDMs with IFNα and analysed transcription levels of the ISGs *Ifit3* and *Cxcl10*. As shown in Fig. 3F, we did not detect differences in *Ifit3* and *Cxcl10* transcript levels between WT and PTP1B$^{-/-}$ BMDMs.

These results suggest that the reduced type I IFN response of PRR-stimulated PTP1B$^{-/-}$ BMDM is neither due to diminished transcription of type I IFNs nor to an impaired feedback loop of the IFNAR.

PTP1B is important for efficient secretion of type I IFNs

Since PTP1B did not affect type I IFN transcription nor the IFNAR signalling pathway in our experimental setup, we hypothesised that it affects either translation or secretion of type I IFNs. Since we also wanted to assess the impact of the phosphatase activity of PTP1B on the type I IFN response, and could not successfully reconstitute primary BMDMs with PTP1B expression constructs, we used Cas9-mediated genetic engineering to generate PTP1B-knockdown (PTP1B^{KD}) immortalised BMDMs (iBMDMs) which can be reconstituted by retroviral transduction. The knockdown of PTP1B was very efficient as shown by immunoblotting of WT and PTP1B^{KD} iBMDMs (Fig. 4A). We then analysed type I IFN levels following cGAS–STING activation of PTP1B^{KD} iBMDMs and observed reduced IFNα levels and unaltered TNFα levels, as in primary PTP1B$^{-/-}$ BMDMs (Fig. 4B; Fig. S2B). We characterised the PTP1B^{KD} iBMDMs further, and analysed activation of the cGAS–STING signalling cascade by immunoblotting, as performed in primary BMDMs (Fig. 3A). As shown in Fig. S2C,D, we observed the same phenotype as was seen in primary BMDMs, namely there was no difference between WT and PTP1B^{KD} iBMDM regarding activation of TBK1 and IRF3 after cGAS stimulation.

Next, we determined whether PTP1B affects (1) translation or (2) secretion of type I IFNs. If PTP1B were important for translation of type I IFNs, we would expect to see a reduction in the total amount of type I IFN in PTP1B^{KD} cells. However, if PTP1B did not affect translation, but rather the secretion of type I IFNs, we would observe an accumulation of intracellular type I IFNs in PTP1B^{KD} cells and lower levels of secreted type I IFNs, while total (intracellular plus secreted) type I IFN production would be unaltered. For this, as schematically depicted in Fig. 4C, we compared (1) secreted type I IFN to (2) intracellular type I IFN and to (3) total levels of type I IFN of WT and PTP1B^{KD} iBMDMs after cGAS activation. Strikingly, we observed higher levels of intracellular IFNα in PTP1B^{KD} iBMDMs compared to WT BMDMs, while levels of secreted IFNα were lower (Fig. 4D), as observed above (Fig. 4B). Consistent with these results, levels of total IFNα (intracellular plus secreted) were equal between PTP1B^{KD} and WT iBMDMs (Fig. 4D). In agreement with our above observations, similar results were obtained upon stimulation of primary BMDMs from WT or PTP1B$^{-/-}$ mice (Fig. S2E).

To confirm our finding that PTP1B supports type I IFN secretion, we labelled stimulated primary BMDMs of WT and PTP1B$^{-/-}$ mice for intracellular IFNβ and performed flow cytometry. To allow for detection of intracellular IFNβ in this manner, we had to prevent its secretion. To do this, we stimulated the cells with 5′ppp-dsRNA or through MCMV infection in the presence of brefeldin A, which blocks the secretion of cytokines by disrupting ER-to-Golgi trafficking. In agreement with our results shown in Fig. 4D, we observed no difference in intracellular IFNβ levels (in this case total IFNβ levels due to the block of secretion by brefeldin A) between WT and PTP1B$^{-/-}$ BMDMs (Fig. 4E), indicating that prevention of secretion leads to the rescue of the phenotype of PTP1B$^{-/-}$ BMDMs.

In conclusion, these results suggest that PTP1B does not affect the translation of type I IFN proteins, but rather is a positive regulator of type I IFN secretion.

The ER localisation of PTP1B, but not its phosphatase activity, is critical for its effect on type I IFN secretion

The phosphatase activity of PTP1B has been shown to be important for its regulation of receptor tyrosine kinases (Stuible and Tremblay, 2010) and most, if not all, its other functions. Since PTP1B is a highly desirable drug target due to its role in obesity, many inhibitors have been identified over recent years, all of which target its phosphatase activity. Therefore, it was important to verify whether the phosphatase activity of PTP1B determines its positive regulatory effect on type I IFN secretion. To do this, we reconstituted PTP1B^{KD} iBMDMs with N-terminally HA-tagged versions of WT PTP1B or with PTP1B carrying a point mutation in the catalytic domain, either D181A or C215S, or the double mutant D181A-C215S, thereby disrupting its phosphatase activity (Ozek et al., 2014; Xie et al., 2002).

PTP1B is anchored to the cytosolic face of the ER membrane via the final 28 to 35 amino acids (aa) of its C-terminal domain (aa 398–432 or 405–432) (Anderie et al., 2007; Frangioni et al., 1992). Hence, we additionally constructed two C-terminal truncation mutants, PTP1B 1-397 and PTP1B 1-404, with the aim of determining whether the subcellular localisation of PTP1B determines its function.

Expression of the phosphatase and membrane anchor mutants was verified by immunoblotting with a PTP1B-specific antibody, which revealed that expression levels of these PTP1B constructs were similar (Fig. 5A). Next, we verified their subcellular localisation by immunofluorescence with an anti-HA antibody, using the ER chaperone calnexin as a marker for the ER. As expected from

Journal of Cell Science (2021) 134, jcs246421. doi:10.1242/jcs.246421

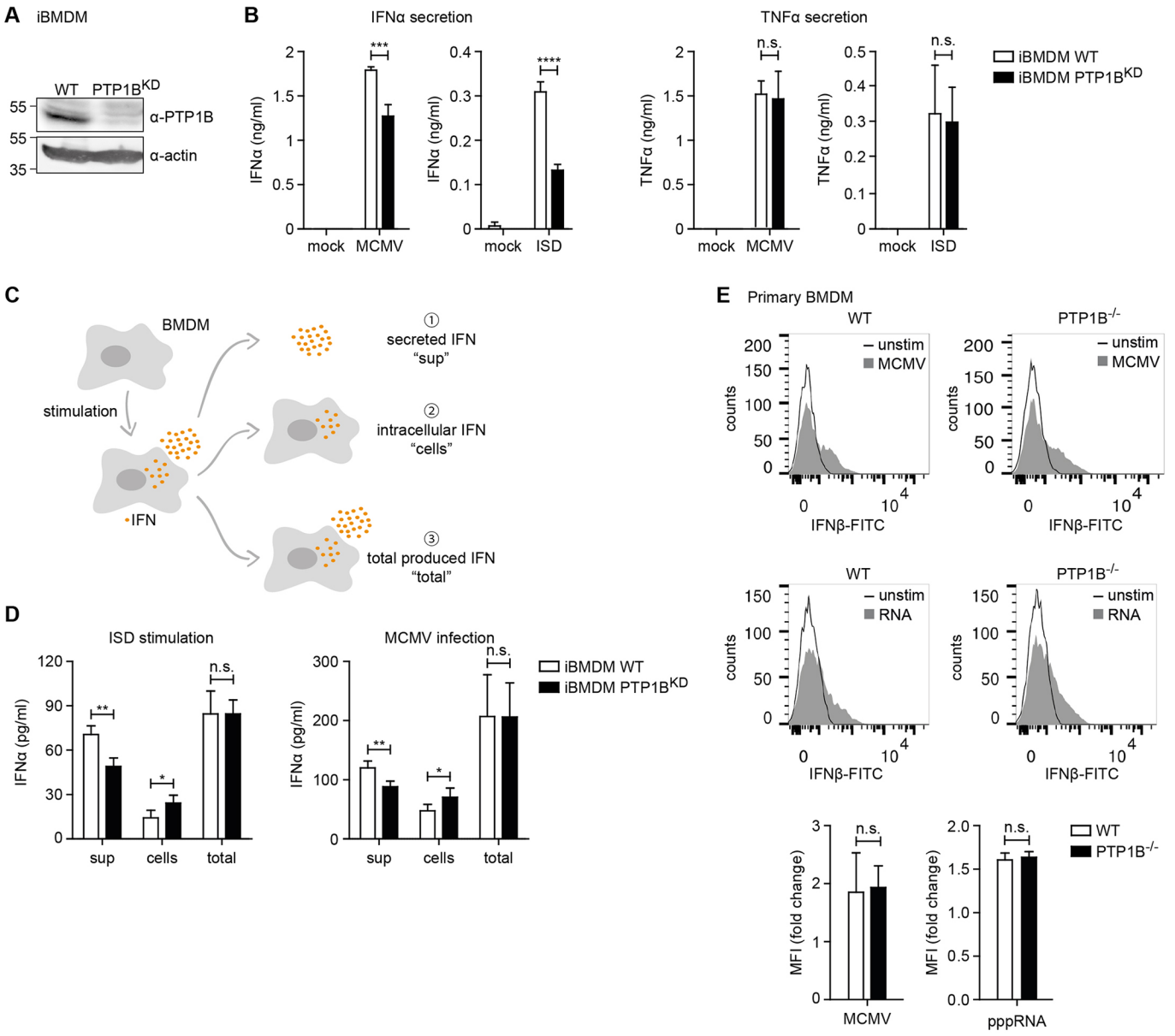

Fig. 4. PTP1B is important for efficient secretion of type I IFN. (A) Cas9-mediated knockdown (KD) of PTP1B in iBMDMs was confirmed by immunoblotting with a PTP1B-specific antibody. (B) WT or PTP1B^{KD} iBMDMs were infected with MCMV at an MOI of 0.5 or transfected with 3 µg/ml ISD. At 16 h post infection or stimulation, levels of IFNα (left panel) or TNFα (right panel) in supernatants were determined by ELISA. Data is shown as mean±s.d. of two combined experiments performed with biological duplicates. Mock samples were treated with either medium only (MCMV panels) or Lipofectamine only (ISD panels). (C) Schematic representation of the experimental setup to measure intracellular type I IFN and total type I IFN production upon stimulation of iBMDMs. At 4 h post stimulation or infection, levels of (1) secreted IFNα in the supernatant (sup), (2) intracellular IFNα (cells) and (3) total IFNα production (total) were determined by ELISA. (D) WT or PTP1B^{KD} iBMDMs were stimulated by transfection with 3 µg/ml ISD or infected with MCMV (MOI 2). At 4 h post stimulation or infection, the supernatant (sup), cells or both combined (total) as described in C were harvested, and IFNα levels were determined by ELISA. Data is shown as mean±s.d. of two combined experiments performed with biological duplicates. (E) Primary BMDMs of WT and PTP1B$^{-/-}$ mice were left untreated (unstim), infected with MCMV or transfected with 3 µg/ml 5′ppp-dsRNA (RNA). After 2 h, 5 µg/ml of brefeldin A were added to prevent cytokine secretion. At 6 h after the addition of brefeldin A, cells were fixed, permeabilised and labelled with a FITC-conjugated antibody against murine IFNβ. Levels of intracellular IFNβ were determined by flow cytometry. Histograms show results from one representative experiment (upper panel, MCMV infection; lower panel, RNA stimulation). Bar graphs show the mean fluorescence intensities (MFI) as mean±s.d. of four or five independent experiments for 5′ppp-dsRNA or MCMV, respectively. Fold change was calculated relative to untreated cells, respectively. *P<0.05; **P<0.01; ***P<0.001; ****P<0.0001; n.s., not significant (unpaired two-tailed Student's t-test).

published studies (Frangioni et al., 1992, Woodford-Thomas et al., 1992), WT PTP1B and PTP1B phosphatase mutants colocalised with calnexin, exhibiting the typical reticular pattern of the ER network (Fig. 5B). In contrast, both PTP1B mutants lacking the ER membrane anchor showed a diffuse cytosolic distribution (Fig. 5B).

Next, we assessed the capacity of WT PTP1B, its phosphatase mutants and its membrane anchor mutants to reconstitute the reduced type I IFN secretion in PTP1B^{KD} iBMDMs upon cGAS–STING stimulation. For all stimuli tested, namely MCMV (Fig. 5C), cGAMP (Fig. 5D) and ISD (Fig. 5E), we saw reduced IFNα and IFNβ secretion in PTP1B^{KD} iBMDMs as demonstrated previously (Fig. 4B). This reduction in type I IFN secretion was rescued in PTP1B^{KD} iBMDMs expressing WT PTP1B (Fig. 5C–E). While the phosphatase mutants D181A and C215S, as well as the double

Journal of Cell Science (2021) 134, jcs246421. doi:10.1242/jcs.246421

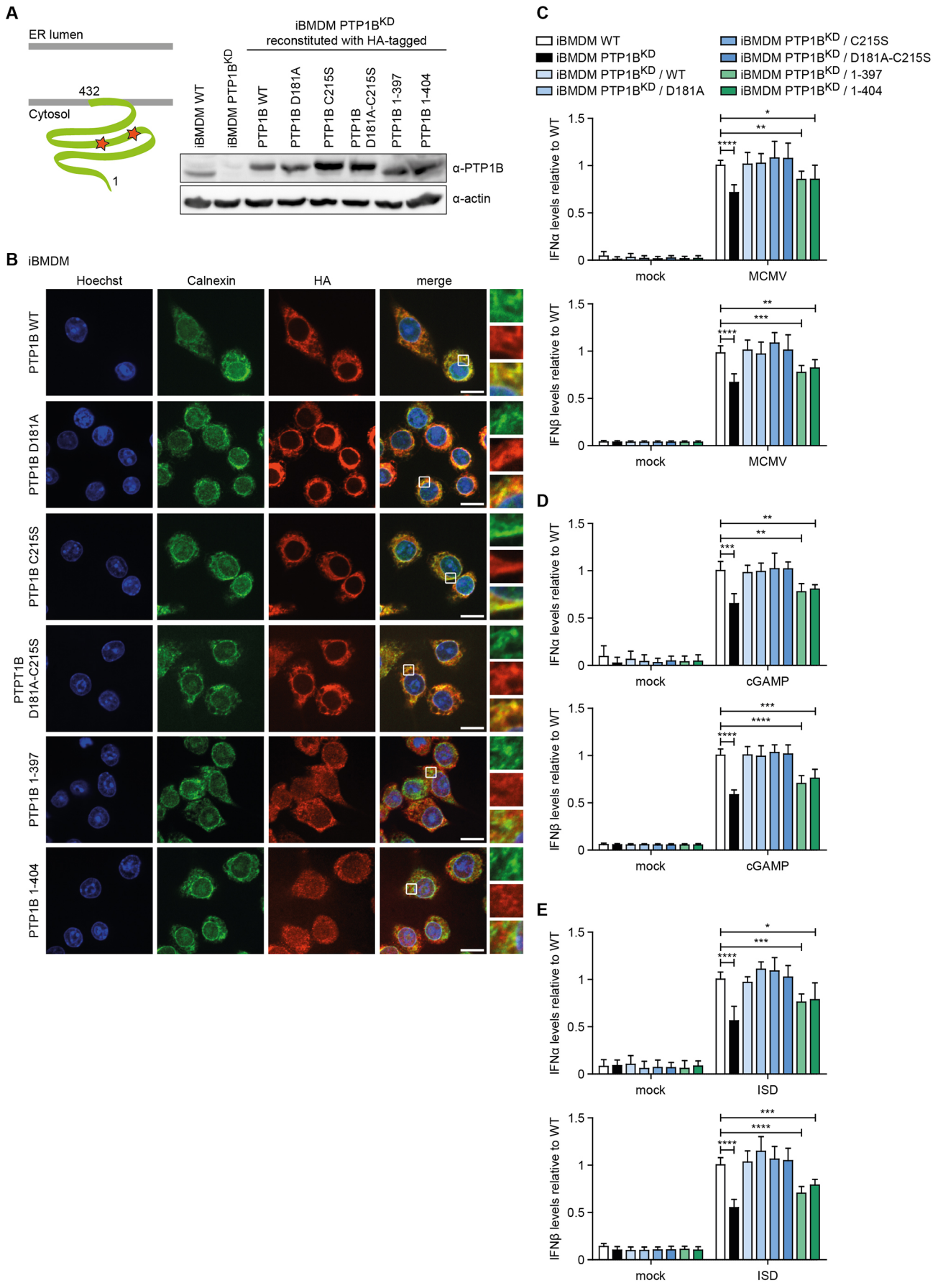

Fig. 5. See next page for legend.

Journal of Cell Science

Fig. 5. Localisation of PTP1B at the ER membrane, but not its phosphatase activity, is required for its complete positive effect on type I IFN secretion. (A) Schematic representation of the PTP1B topology with the two red stars indicating the amino acid positions D181 and C215, which are crucial for its phosphatase activity. Immortalised PTP1B^{KD} BMDMs were reconstituted with HA-tagged versions of PTP1B WT, the phosphatase-inactive mutants D181A, C215S or D181A-C215S, or mutants lacking the ER anchor, PTP1B 1-397 or PTP1B 1-404. Expression of endogenous PTP1B and its HA-tagged versions was determined by immunoblotting with a PTP1B-specific antibody. (B) Expression of the PTP1B mutants described in A in iBMDM PTP1B^{KD} was analysed by immunofluorescence with an HA antibody by confocal microscopy. The ER was visualised with an antibody to the ER marker calnexin, and nuclei were stained with Hoechst 33342. White boxes indicate the region shown at a higher magnification. Scale bars: 10 µm. (C–E) WT iBMDMs, PTP1B^{KD} iBMDMs and PTP1B^{KD} iBMDMs stably expressing either HA-tagged PTP1B WT, D181A, C215S, D181A-C215S, 1-397 or 1-404 were infected with either MCMV at an MOI of 2 (C) or stimulated by addition of 10 µg/ml cGAMP (D) or by transfection of 3 µg/ml ISD (E). At 16 h post infection or stimulation, levels of IFNα (upper panel) and IFNβ (lower panel) in supernatants were determined by ELISA. Mock samples were treated with either medium only (MCMV and cGAMP panels) or Lipofectamine only (ISD panels). Results are shown as mean±s.d. normalised to secreted levels of stimulated WT iBMDM combined from three independent experiments performed with biological duplicates. *P<0.05, **P<0.01, ***P<0.001, ****P<0.0001 (unpaired two-tailed Student's t-test). Differences between datasets were not significant if not stated otherwise.

mutant D181A-C215S, showed the same phenotype as WT PTP1B, PTP1B lacking its membrane anchor and therefore losing its ER localisation, could not restore type I IFN secretion (Fig. 5C–E). Again, as observed in primary BMDMs (Figs 2F and 3B–D), neither transcription of *Ifnb1* (Fig. S3A) nor TNFα secretion (Fig. S3B) was affected in PTP1B^{KD} iBMDMs or any of the reconstituted iBMDM cell lines.

These results unequivocally show that the phosphatase activity of PTP1B is dispensable for type I IFN secretion, while attachment to the ER membrane is crucial for the positive impact of PTP1B on type I IFN secretion.

PTP1B is important for the type I IFN response upon TLR stimulation and MCMV infection in the host

So far, we have shown that PTP1B plays a role for optimal type I IFN secretion *in vitro* in primary cells (pDCs and BMDMs) as well as immortalised BMDM. Next, we wanted to assess the impact of PTP1B *in vivo* in the context of TLR stimulation and MCMV infection.

First, we stimulated the TLR response *in vivo* by injecting the synthetic TLR9 agonist CpG DNA and included TLR9$^{-/-}$ mice as specificity control. In addition, we verified that PTP1B$^{-/-}$ mice have the same numbers of conventional DCs (cDCs) and pDCs as WT mice since pDCs are the main producers of type I IFNs (Fig. S4A).

Recapitulating our *in vitro* findings, PTP1B$^{-/-}$ mice showed reduced IFNα levels in the serum upon TLR9 stimulation, but equal levels to those in TNFα as WT mice, while IFNα and TNFα were not detected in TLR9$^{-/-}$ mice (Fig. 6A). We obtained the same results in the context of MCMV infection (Fig. 6B), where we used STING$^{-/-}$ mice as a control for the early [6 h post infection (h.p.i.)] type I IFN response, since STING is essential for this initial type I IFN response to MCMV (Stempel et al., 2019; Lio et al., 2016). We also observed reduced type I IFN levels at a later time point (36 h) post MCMV infection, with 3d mice as a control, since they lack endosomal TLR signalling which is crucial for type I IFN secretion at this later time point post MCMV infection (Fig. S4B). Notably, *Ifnb1* transcription was not reduced in PTP1B$^{-/-}$ mice (Fig. S4C). These results clearly recapitulate our *in vitro* findings showing that PTP1B acts downstream of multiple PRRs (cGAS and endosomal TLRs) and that it affects production of type I IFNs at the post-transcriptional level.

Consistent with the reduced type I IFN response in PTP1B$^{-/-}$ mice, we saw a modest, but significant, increase in MCMV immediate early 1 (*IE1*) and early 1 (*E1*) transcript levels in the spleens of PTP1B$^{-/-}$ mice at 6 h post infection (Fig. 6C), as well as in primary BMDM of PTP1B$^{-/-}$ mice at 2 and 4 h post infection (Fig. S4D). As observed in our previous study (Stempel et al., 2019), MCMV transcripts were reduced in STING$^{-/-}$ mice since the STING-mediated NF-B response supports transcription of MCMV genes (Fig. 6C).

In conclusion, we have shown that PTP1B is a positive regulator of the type I IFN response downstream of the PRRs TLR9 and cGAS–STING *in vivo*, and that the reduced type I IFN response in PTP1B$^{-/-}$ mice leads to elevated MCMV transcript levels.

DISCUSSION

Here, we have provided evidence that the tyrosine phosphatase PTP1B is involved in efficient secretion of type I IFN, and that this function of PTP1B is independent of its phosphatase activity, but requires its localisation to the ER. The requirement for PTP1B to be attached to the cytosolic face of the ER membrane to regulate type I IFN secretion would be in line with the hypothesis that PTP1B is involved in trafficking events of type I IFN from the ER to the Golgi, endosomes or the plasma membrane.

PTP1B is known for its prominent role for receptor tyrosine kinase trafficking and signalling (Través et al., 2014; Abdelsalam et al., 2019; Hughes et al., 2015; Vieira et al., 2017). As we had originally identified PTP1B in affinity purification coupled to mass spectrometry analyses as being associated with the ER membrane protein UNC93B, we first hypothesised that PTP1B regulated trafficking or signalling of the UNC93B–TLR complex from the ER to endosomes, from where TLRs activate a signalling cascade leading to transcription of cytokines. Indeed, we could demonstrate that PTP1B plays a role in innate immune signalling, but it acts downstream of multiple PRRs and not only downstream of UNC93B-dependent TLRs. We observed that PTP1B positively regulates the type I IFN response mediated by the DNA sensor cGAS and the RNA sensor RIG-I. Furthermore, we demonstrated that PTP1B does not regulate PRR-mediated induction of type I IFN transcription, nor signalling of the IFNAR leading to ISG transcription, but that it is involved in efficient secretion of type I IFNs, which links back to its well-established function as a regulator of trafficking events.

Notably, all other functions of PTP1B that are described in the literature are strictly dependent on its phosphatase activity, and these studies show that PTP1B is a negative regulator of insulin and leptin signalling (Tonks, 2013; Feldhammer et al., 2013), EGFR signalling (Hughes et al., 2015; Young and Kim, 2019), IFNAR signalling (Myers et al., 2001; Carbone et al., 2012) and TLR signalling (Xu et al., 2008). Only a few studies have addressed the role of PTP1B in the context of the innate immune response in macrophages or *in vivo*, and none has addressed its role in the context of viral infection. The only study that addressed the role of PTP1B in the context of infection in mice was reported by Yue and colleagues who showed that PTP1B has a negative impact on the host response to infection with the bacterium *Pseudomonas aeruginosa* (Yue et al., 2016). However, this experimental system is very different from our infection system with the herpesvirus MCMV and cannot be compared directly. Another study mainly focused on the pro- and anti-inflammatory response of macrophages, and found that PTP1B deficiency increases the

Journal of Cell Science (2021) 134, jcs246421. doi:10.1242/jcs.246421

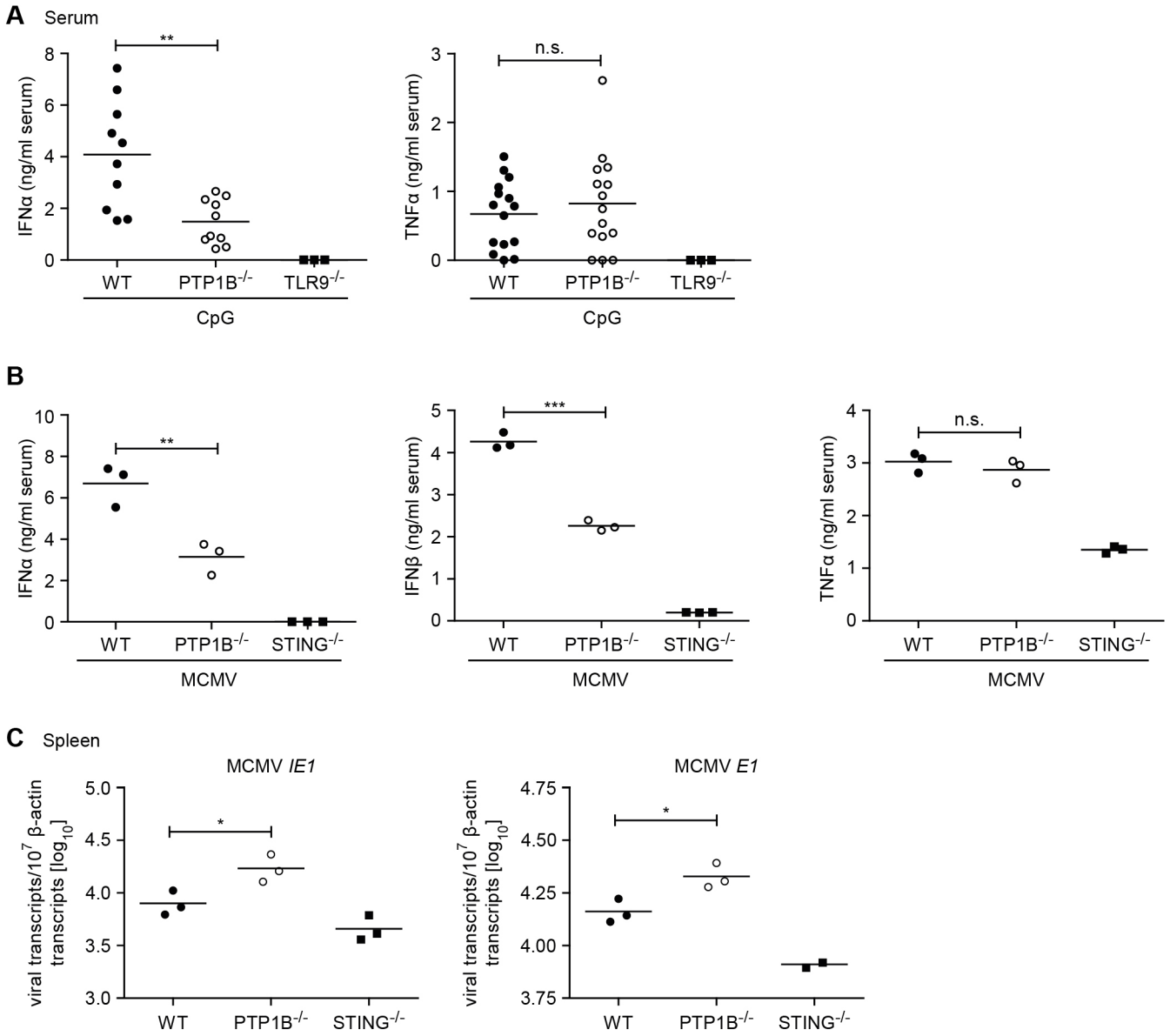

Fig. 6. The type I IFN, but not the TNFα response, is impaired in PTP1B$^{-/-}$ mice. (A) WT, PTP1B$^{-/-}$ or TLR9$^{-/-}$ mice were intravenously injected with CpG DNA. Serum levels of IFNα (left panel) were determined by ELISA 6 h post injection. To determine TNFα levels, mice were intraperitoneally injected with CpG DNA. After 2 h, serum was collected and subjected to TNFα ELISA (right panel). (B) WT, PTP1B$^{-/-}$ and STING$^{-/-}$ mice were intravenously infected with 4×10^5 PFU MCMV. At 6 h post infection, serum levels of IFNα (left panel), IFNβ (centre panel) and TNFα (right panel) were determined by ELISA. (C) WT, PTP1B$^{-/-}$ and STING$^{-/-}$ mice were intravenously infected with 4×10^5 PFU MCMV. After 6 h, total RNA was extracted from the spleen and transcript levels of MCMV *IE1* (left panel) and MCMV *E1* (right panel) were determined by qRT-PCR and normalised to β-actin. Each dot represents an individual mouse and black bars indicate the mean value of each group. *P<0.05; **P<0.01; ***P<0.001; n.s., not significant (unpaired two-tailed Student's *t*-test).

effects of proinflammatory challenge (Través et al., 2014). Our study only analysed TNFα and IL6 as pro-inflammatory cytokines, and in our experimental settings we did not see differences in their secretion between WT and PTP1B$^{-/-}$ mice. Since we make consistent observations between iBMDMs with a Cas9-mediated PTP1B knockdown, primary bone marrow cells and primary BMDMs derived from PTP1B$^{-/-}$ mice included littermates as control, and performed *in vivo* studies that are consistent with our *in vitro* findings, we currently do not have an explanation for this discrepancy.

Xu et al. reported a negative role of PTP1B for TLR signalling in RAW264.7 macrophages and HEK293-T cells, as revealed by siRNA-mediated knockdown and PTP1B overexpression experiments (Xu et al., 2008). This phenotype was dependent on the phosphatase activity of PTP1B. Interestingly, when we overexpress PTP1B in HEK 293-T reporter cells, we also see that PTP1B negatively regulates PRR signalling (data not shown). However, in primary cells (pDCs or BMDMs) from PTP1B$^{-/-}$ mice and in iBMDMs with a Cas9-mediated gene knockdown of PTP1B (PTP1B^{KD}) we see the opposite phenotype; PTP1B had a positive impact on PRR signalling. When we reconstitute PTP1B^{KD} iBMDMs with PTP1B expression constructs that express PTP1B at similar levels to endogenous PTP1B (Fig. 5A), we unequivocally show that expression of WT PTP1B rescues the phenotype and that the phosphatase activity of PTP1B is not required for its role in type I IFN secretion (Fig. 5C). We also carefully controlled localisation of our PTP1B mutants and verified their proper ER localisation (WT PTP1B and phosphatase mutants) or their loss of ER localisation (PTP1B 1-397 and 1-404). Overexpression studies in cell lines can

be very useful, but ideally should to be complemented with knockout/knockdown studies in primary cells combined with carefully controlled reconstitution experiments.

Interestingly, our study found that PTP1B selectively regulates type I IFN signalling, while TNFα secretion was not affected in PTP1B-deficient cells. While numerous studies describe the signalling pathways that lead to cytokine expression and the pathways that are induced by cytokines and their respective receptors, the pathways and mechanisms of cytokine trafficking and release in different cell types are still poorly understood. Some gains have been made in understanding the secretion of cytokines such as interleukins and TNFα (Murray and Stow, 2014; Lacy and Stow, 2011); however, virtually nothing is known regarding type I IFNs. Notably, the intracellular pathways available for release are often uniquely tailored to each cytokine and cell type (Manderson et al., 2007), which could explain our finding that PTP1B affects type I IFN but not TNFα secretion.

A couple of scenarios are possible to explain how PTP1B could regulate type I IFN trafficking or release from cells. For instance, it might be involved in the classical secretion pathway and contribute to vesicle formation for the transport of type I IFNs from the ER to the Golgi, where they are further processed and then, at the trans Golgi network (TGN), loaded into vesicles for delivery to the plasma membrane. Direct vesicle transport from the ER to recycling endosomes is also a possibility. Given the observation that PTP1B requires localisation to the ER to promote type I IFN secretion, another possibility is that type I IFNs are secreted via ER–plasma membrane contact sites. The ER exists as an elaborate membrane network (Nixon-Abell et al., 2016; Guo et al., 2018) that extends throughout the cytosol and forms stable contacts with nearly all other organelles (Wu et al., 2018). PTP1B interacts with the endocytosed EGFR at contact sites between the ER and multivesicular bodies (Eden et al., 2010). The original function of contact sites between the ER and membranes of the Golgi, endosomes and plasma membrane was described to be the transfer of lipids and Ca^{2+} ions, but today it is clear that the diversity of their functions is much broader (Scorrano et al., 2019). It may be possible that PTP1B, being located at such contact sites, interacts with other cellular proteins that regulate trafficking of type I IFN, or that PTP1B functions as a tether to bring the ER and plasma membrane in close proximity in PRR-stimulated cells (Eisenberg-Bord et al., 2016), but this hypothesis is highly speculative at this point.

Since many trafficking molecules are tightly coupled to cell activation and respond to the need for cytokine secretion through upregulation of their expression (Low et al., 2010; Stow et al., 2006), it would be interesting to analyse the proteome of macrophages with an activated cGAS–STING pathway for upregulation of proteins involved in trafficking events such as ADP-ribosylation factors, Rab GTPases or SNAREs. However, this would ideally be analysed specifically for type I IFNs, but the PRR signalling pathways leading to type I IFN induction are difficult to separate from the ones leading to proinflammatory cytokine induction via NF-κB. Alternatively, a genome-wide Cas9 screen for proteins involved in type I IFN, but not TNFα or IL6 secretion, may reveal more players specific for type I IFN secretion.

The studies on type I IFN trafficking and release are clearly hampered by a lack of suitable antibodies for immunoblotting and immunofluorescence studies that are sensitive enough to detect the low concentration of these cytokines within the different cellular compartments at a snapshot in time. Cytokine secretion by nature has to be an efficient and fast process in order to quickly respond to infection. Attempts to fuse IFNβ with fluorescent proteins, which would allow researchers to investigate its trafficking, have not been reported or did not succeed (Stefan Lienenklaus, personal communication), which is not surprising since the addition of a large protein such as GFP may negatively affect IFNβ trafficking. Hence, with the identification of PTP1B as a positive regulator of type I IFN signalling, we have gained an insight into the mechanisms of type I IFN trafficking and secretion.

Since PTP1B is an attractive therapeutic target owing to its role in type II diabetes and obesity, understanding the cellular mechanisms modulated by PTP1B is of crucial importance. While we found that PTP1B does not depend on its phosphatase activity to promote type I IFN secretion, there is merit in investigating the potential side effects posed by PTP1B inhibitors, which are lead candidates for clinical trials on innate immune responses. While we did not observe a strong effect of PTP1B on MCMV replication in its host, this may not hold true for other pathogens.

Collectively, we have revealed a positive regulatory role for PTP1B in PRR-mediated innate immune responses in macrophages in the context of viral infection. Further investigations into how PTP1B specifically regulates the type I IFN response will contribute greatly to the understanding of the molecular mechanisms behind the elusive nature of type I IFN secretion.

MATERIALS AND METHODS

Ethics statement

All animal experiments were performed in compliance with the German animal protection law (TierSchG BGBI S. 1105; 25.05.1998). The mice were handled in accordance with good animal practice as defined by FELASA and GV-SOLAS. All animal experiments were approved by the responsible state office (Lower Saxony State Office of Consumer Protection and Food Safety) under permit numbers #33.19-42502-04-12/0930 and #33.19-42502-04-17/2657.

Mice

WT and knockout mice were bred and maintained under specific-pathogen-free conditions at the animal facility of the Helmholtz Centre for Infection Research (HZI) in Braunschweig, Germany. WT C57BL/6J were originally obtained from Charles River Laboratories. PTP1B$^{-/-}$ mice [B6.129S4-Ptpn1(tm1Bbk)/Mmjax], backcrossed 20× to C57BL/6J mice, were obtained from the Jackson Laboratory (MMRRC, stock number: 032240-JAX) (Klaman et al., 2000). Tlr9$^{-/-}$ (B6.129P2-Tlr9^{tm1Aki}) mice (Hemmi et al., 2000) were backcrossed to C57BL/6J mice for 12 generations and obtained from Stefan Bauer, University of Marburg, Germany. STING$^{-/-}$ mice (*MPYS*$^{-/-}$/Tmem173$^{tm1.2Camb}$) (Jin et al., 2011) were kindly provided by Bastian Opitz, Charité Berlin, Germany, with permission of Lei Jin, University of Florida, USA. The 3d mutation introduces a positively charged residue into the ninth of twelve transmembrane domains (H412R) of UNC93B1 (Tabeta et al., 2006). This abrogates binding of UNC93B1 to endosomal TLRs and their retention in the ER, resulting in abolished endosomal TLR signalling (Tabeta et al., 2006; Brinkmann et al., 2007). MAVS$^{-/-}$ mice (Michallet et al., 2008) were kindly provided by Ulrich Kalinke, Twincore, Hannover. IFNβ reporter mice (Ifnb1$^{tm1.2Lien}$) were as described previously (Lienenklaus et al., 2009; Solodova et al., 2011). These mice were crossed as heterozygotes (IFNβ$^{+/Δβ\text{-}luc}$) with either PTP1B$^{-/-}$ or STING$^{-/-}$ mice to obtain PTP1B$^{-/-}$/IFNβ$^{+/Δβ\text{-}luc}$ and STING$^{-/-}$/IFNβ$^{+/Δβ\text{-}luc}$ mice, respectively. Mice used in this study were 8–10 weeks old and female.

Viruses

MCMV-GFP has been previously described (Mathys et al., 2003). WT MCMV for *in vitro* infection experiments is the MCK-2-repaired BAC-derived MCMV (Jordan et al., 2011). MCMV Δm157 for *in vivo* infection experiments was kindly provided by Stipan Jonjic (Faculty of Medicine, University of Rijeka, Croatia) and recently described in Stempel et al. (2019). Newcastle disease virus (NDV) was kindly provided by Andrea Kröger (Otto-von-Guericke University Magdeburg, Germany).

Primary cells

For generation of total bone marrow cells, bone marrow extracted from mice was subjected to red blood cell lysis before culturing in RPMI medium supplemented with 10% FCS, 2 mM glutamine (Gln), 1% penicillin-streptomycin (P/S) and 50 µM β-mercaptoethanol. For generation of primary bone marrow-derived macrophages (BMDMs), the bone marrow was extracted from mice and the cells were cultured in DMEM (high glucose) supplemented with 10% FCS, 2 mM Gln, 1% P/S, 50 µM β-mercaptoethanol and 5% macrophage colony stimulating factor (MCSF) as described previously (Bussey et al., 2014).

Cell lines

The immortalised murine bone marrow-derived macrophage (iBMDM) cell line was obtained through BEI Resources, NIAID NIH (NR-9456). iBMDMs were maintained in DMEM supplemented with 8% FCS, 2 mM Gln, 1% P/S and 50 µM β-mercapthoethanol.

To generate PTP1^{KD} iBMDMs, a guide RNA targeting the second exon of PTP1B was cloned into the pLK05 gRNA vector (kindly provided by Dirk Heckl, Hannover Medical School, Germany), which expresses a single gRNA, SpCas9 and an RFP reporter. gRNA sense and antisense oligonucleotides were ordered (IDT) and manually annealed. The gRNA sequence is as follows: PTP1B gRNA 2-63 FOR, 5′-CACCGTGACATCTCGGTACCTG-TTCM-3′; PTP1B gRNA 2-63 REV: 5′-AAACGAACAGGTACCGAGAT-GTCAC-3′. iBMDM were transduced with lentivirus to stably express Cas9 and the gRNA targeting PTP1B. Cells were selected for red fluorescence by FACS. For reconstitution of PTP1B in PTP1B^{KD} iBMDMs, HA-tagged PTP1B WT was cloned into pMSCVpuro using the *Bgl*II/*Eco*RI restriction sites. Mutations or deletions in PTP1B to generate PTP1B D181, C215S, D181A-C215S, 1-397 or 1-404 were carried out using the Q5® Site Directed Mutagenesis kit (NEB, #E0554). PTP1B^{KD} iBMDMs stably expressing HA-tagged WT PTP1B or mutant PTP1B were generated by retroviral transduction using the respective constructs in the pMSCVpuro vector and selection with 10 µg/ml puromycin. Knockdown of PTP1B and reconstitution with the respective mutant was verified by immunoblotting. All cell lines used in this study have been tested for contamination.

Antibodies and reagents

To determine the percentages of cDC and pDC in bone marrow and inguinal lymph nodes by flow cytometry, the following set of antibodies was used: anti-Siglec-H-APC (#51-0333-82, dilution 1:1000), anti-CD11b-PE (#12-0112-82, dilution 1:4000), and anti-CD45R/B220-PerCP-Cy5.5 (#45-0452-82, dilution 1:500) from eBioscience, anti-CD11c-PE/Cy7 (#117318, dilution 1:1000) from BioLegend, and anti-mPDCA-1-FITC (#130-091-961, dilution 1:10) from Miltenyi Biotec. Anti-CD11b-FITC (#557396, dilution 1:200) from BD Biosciences and anti-F4/80-PE (#123110, dilution 1:100) from BioLegend were used for phenotype analysis of BMDM by flow cytometry. Recombinant mouse IFNα (#12100, dilution 1:10) and anti-IFNβ-FITC (#22400-3, Clone RMMB-1, dilution 1:10) were purchased from PBL Assay Science. Rabbit anti-STING (#13647, clone D2P2F, dilution 1:1000), rabbit anti-phospho-TBK1 (#5483, clone D52C2, dilution 1:1000), rabbit anti-phospho-IRF3 (#4947, clone 4D4G, Ser396, dilution 1:1000), were purchased from Cell Signaling. Rabbit anti-IRF3 (#sc-9082, clone FL-425, dilution 1:2000) was obtained from Santa Cruz Biotechnology. Mouse anti-tubulin (#T6199, clone DM1A, dilution 1:1000), mouse anti-actin (A5441, clone AC-15, dilution 1:5000) and rabbit anti-calnexin (C4731, dilution 1:10,000) were obtained from Sigma-Aldrich. Mouse anti-HA antibody was obtained from Covance (MMS-191R, clone 16B12, dilution 1:1000). Antibodies against PTP1B were purchased from Millipore (ABS40, dilution 1:500) or Abgent (AM8411a, dilution 1:100) and specificity was verified by testing lysates of *PTP1B*$^{-/-}$ BMDM. HRP-conjugated secondary antibodies were purchased from Dianova.

CpG 2336, CpG 1826, CpG 2216 and interferon stimulatory DNA (ISD) were obtained from Eurofins Genomics. ISD was generated by the combination of complementary forward (ISD45bp-for: 5′-TACAGATCT-ACTAGTGATCTATGACTGATCTGTACATGATCTACA-3′) and reverse (ISD45bp-rev: 5′-TGTAGATCATGTACAGATCAGTCATAGATCACT-AGTAGATCTGTA-3′) 45 bp oligonucleotides, heating to 95°C for 10 min followed by annealing at room temperature. Poly(U) (#tlrl-sspu), 5′ppp-dsRNA (#tlrl-3prna) and 2′3′-cGAMP (#tlrl-nacga23) were obtained from Invivogen. Protease inhibitors (#4693116001), phosphatase inhibitors (#4906837001) and DOTAP Liposomal Transfection Reagent were purchased from Roche. Lipofectamine 2000 and OptiMEM were purchased from Thermo Fisher Scientific.

Stimulation of cells for ELISA

10^6 total bone marrow cells or 1.5×10^5 BMDMs were seeded per well in 96-well plates. Cells were incubated with stimuli or infected with MCMV-GFP in a total volume of 200 µl per well. For stimulation with poly(U), cells were transfected with 200 ng of poly(U) and 1.2 µl of DOTAP diluted in HBS (20 mM HEPES pH 7.4 and 150 mM NaCl) according to the manufacturer's instructions. For stimulation with CpG 2336, the stimulus was added to the samples to a final concentration of 1 µM. For stimulation with ISD or 5′ppp-dsRNA, BMDMs were stimulated by transfection with either 1 or 3 µg/ml ISD or 1 or 3 µg/ml 5′ppp-dsRNA complexed with Lipofectamine, as indicated, or transfected with Lipofectamine only as control. 2′3′-cGAMP was added to the medium to a final concentration of 10 µg/ml or cells were stimulated by transfection with 3 µg/ml cGAMP complexed with Lipofectamine. Supernatants were harvested at indicated time points and stored at −20°C for ELISA.

In vivo experiments

To analyse type I IFN induction *in vivo*, mice were intravenously injected with a total volume of 200 µl containing 10 µg CpG 2216 complexed with 30 µl DOTAP in PBS and mice were killed 6 h later. To measure TNFα responses, mice were intraperitoneally injected with 60 µg of CpG 1826 in a total volume of 200 µl in PBS and mice were killed at 2 h post injection. For MCMV infection, mice were intravenously infected with 4×10^5 plaque-forming units (PFU) of recombinant MCMV and killed at 6 or 36 h post infection. Blood was kept at RT for at least 1 h and centrifuged for 8 min at 2400 ***g***. Serum supernatants were collected and stored at −20°C for ELISA. The preparation of serum, spleen and liver samples from infected mice for measuring type I IFN levels by ELISA and for *Ifnb1* mRNA by qRT-PCR has been described previously (Stempel et al., 2019; Chan et al., 2017).

ELISA

IFNα levels were measured as described previously (Bussey et al., 2019). IFNβ was detected using the LEGEND MAX Mouse IFN-β ELISA Kit (BioLegend, #439407) or the LumiKine™ Xpress mIFN-β kit (Invivogen, #luex-mifnb) according to the manufacturer's instructions. IL6 was detected using the Mouse IL6 ELISA Set (BD Biosciences, #555240) according to the manufacturer's instructions. Levels of TNFα were determined as described previously (Bussey et al., 2014).

Detection of intracellular IFNα by ELISA

BMDMs were stimulated as described above in quadruplicates. At the indicated time points, the supernatants were harvested from two wells. To these wells, 100 µl of fresh medium were added, and cells were scraped from the plate to obtain the 'cells only' sample. From the corresponding two remaining wells, cells were scraped in the supernatant to analyse the total amount of cytokines produced. Triton X-100 (Sigma) was added to all samples to a final concentration of 0.1% Triton X-100, and solutions were incubated on ice for 15 min to disrupt the cells, followed by centrifugation for 5 min at 4°C and 14,000 ***g***. After centrifugation, the supernatants were transferred into a new tube for analysis by ELISA. Secreted, intracellular and total IFNα was measured with the LumiKine™ Xpress mIFN-α kit (Invivogen, #luex-mifna) according to the manufacturer's instructions.

Flow cytometry

To determine the proportions of cDCs and pDCs, bone marrow and inguinal lymph nodes were prepared from WT and PTP1B$^{-/-}$ mice, collected in RPMI medium and passed through a 100 µm cell strainer. Bone marrow cells were subjected to red blood cell lysis. Cells were incubated with Mouse Fc Block (BD Biosciences, #553141) diluted in PBS for 10 min, and stained with antibodies for CD11c, CD11b, B220, Siglec-H and mPDCA-1 diluted in PBS for 15 min. Dead cells were stained with the LIVE/DEAD Fixable Aqua Dead Cell stain kit (Invitrogen, #L34957) according to the

manufacturer's instructions, and cells were resuspended in PBS for analysis. All steps were carried out at 4°C.

For phenotype analysis of BMDMs, cells were incubated with Mouse Fc Block diluted in FACS buffer (PBS with 2% FCS) for 10 min and stained with antibodies for CD11b and F4/80 diluted in FACS buffer for 15 min. Cells were resuspended in FACS buffer for analysis. All steps were carried out at 4°C.

To measure intracellular IFNβ, 1.5×10^5 BMDMs were seeded per well in six-well plates. For stimulation with 5′ppp-dsRNA, cells were transfected with 3 µg of RNA and 5 µl of Lipofectamine diluted in OptiMEM in a total volume of 1 ml per well. For infection with MCMV, the diluted virus was added to the cells at a multiplicity of infection (MOI) of 1 in a total volume of 2.5 ml per well and plates were centrifuged for 5 min at 684 ***g*** to enhance infection. At 2 h after stimulation, 5 µg/ml of brefeldin A (Sigma-Aldrich, #B7651) were added to the cells. At 6 h after the addition of brefeldin A, cells were washed with PBS and transferred to 96-well plates. Cells were fixed with 4% paraformaldehyde for 10 min, washed with PBS twice, resuspended in PBS and stored overnight at 4°C for antibody staining. Fixed cells were permeabilised with 0.5% saponin in FACS buffer (FACS-S) for 20 min and stained with a FITC-conjugated anti-mouse IFNβ antibody diluted in FACS-S buffer for 1 h. Cells were washed with FACS-S buffer twice and resuspended in FACS buffer for analysis. Permeabilisation and antibody staining were carried out at 4°C.

Flow cytometry data was acquired using a LSR II flow cytometer and FACSDiva software (BD Biosciences). Data was analysed with FlowJo software (Version 10, Tree Star, Inc.).

Luciferase-based reporter assay

1.5×10^5 BMDMs were seeded per well in 96-well plates. Cells were transfected with 600 ng of 2′3-cGAMP and 1 µl of Lipofectamine diluted in OptiMEM or infected with MCMV-GFP at the indicated MOIs in a total volume of 200 µl per well. After 3 h, cells were lysed in 50 µl of 1× Luciferase cell culture lysis reagent (Promega) per well. Luciferase production was measured using the Dual-Luciferase® Reporter Assay System (Promega, #E1960) and a GloMax 96 Microplate Luminometer (Promega).

Immunoblotting

For analysis of the activation of the cGAS-STING signalling cascade by immunoblotting for phosphorylated TBK1 and IRF3, 3.5×10^5 primary BMDMs from WT or $PTP1B^{-/-}$ mice, or iBMDM or $PTP1B^{KD}$ iBMDM cells were seeded in a 12-well plate. Cells were either infected with MCMV-GFP at an MOI of 0.5 or stimulated by transfection with 10 µg/ml ISD complexed with Lipofectamine, or treated with Lipofectamine only. At the indicated times, cells were lysed in RIPA buffer (20 mM Tris-HCl pH 7.5, 1 mM EDTA, 100 mM NaCl, 1% Triton X-100, 0.5% sodium deoxycholate and 0.1% SDS) containing protease and phosphatase inhibitors (Roche 4693116001 and 4906837001, respectively). Cell lysates were cleared by centrifugation (14,000 ***g*** for 10 min at 4°C) and supernatants were frozen at −20°C for further analysis.

Cell lysates were separated by SDS-PAGE and transferred onto nitrocellulose or PVDF membrane (GE Healthcare) using wet transfer and Towbin blotting buffer [25 mM Tris-HCl pH 8.3, 192 mM glycine, 20% (v/v) methanol]. Membranes were probed with the indicated primary antibodies and respective secondary HRP-coupled antibodies diluted in 5% w/v nonfat dry milk or 5% BSA (Sigma) in TBS-T. Immunoblots were developed with Lumi-Light (Roche), SuperSignal West Pico or SuperSignal West Femto (Thermo Fisher Scientific) chemoluminescence substrates. Membranes were exposed to films or imaged with a ChemoStar ECL Imager (INTAS) and band intensities were quantified using LabImage 1D software (INTAS). Images were prepared using Adobe Photoshop CS5.

Immunofluorescence

iBMDM (125,000 cells/well) were seeded onto acid-washed coverslips in 24-well plates. After 24 h, cells were permeabilised with ice-cold methanol for 5 min at −20°C followed by fixation with 4% PFA in PBS for 20 min at room temperature. Cells were washed three times with PBS, and then incubated in 10% FCS and 1% BSA in PBS for 1 h at room temperature. Primary antibodies diluted in 1% BSA in PBS were added overnight at 4°C, followed by three PBS washes. Cells were incubated with secondary antibodies coupled to Alexa Fluor 488 or Alexa Fluor 594 and Hoechst 33342 (Thermo Fisher Scientific) diluted in 1% BSA in PBS for 45 min at room temperature. Coverslips were mounted on glass microscope slides with Prolong Gold (Invitrogen). Imaging was performed on a Nikon ECLIPSE Ti-E inverted microscope equipped with a spinning disk device (Perkin Elmer Ultraview), and images were processed using Volocity software (Version 6.2.1, Improvision).

Quantitative RT-PCR

Primary BMDMs or immortalised BMDM s were infected by centrifugal enhancement with MCMV-GFP at an MOI of 0.01, 0.1 or 2, and stimulated by addition of 10 µg/ml cGAMP, 3 µg/ml ISD, 1 µg/ml 5′ppp-dsRNA or 100 U/ml of recombinant mouse IFNα, for 2 or 4 h. Cells were lysed with RLT buffer supplemented with β-mercaptoethanol and RNA was purified with the RNeasy Mini Kit (Qiagen, #7410) followed by DNase treatment (Qiagen, #79254) according to the manufacturer's instructions. Similarly, RNA from spleen and liver homogenates was extracted according to the manufacturer's instructions. For synthesis of cDNA and quantification of *Rpl8*, *Ifnb1*, *Ifit3* and *Cxcl10* gene transcripts, 100 ng of RNA were used per sample and quantitative RT-PCR was performed using the EXPRESS One-Step Superscript™ qRT-PCR kit (Invitrogen, #11781200) on a LightCycler 96 instrument (Roche). *Rlp8* served as the housekeeping control. PCR primers and Universal ProbeLibrary probes (UPL, Roche) were used as follows: *Rlp8* (Rlp8_for, 5′-CAACAGAGCCGTTGTTGGT-3′; Rlp8_rev, 5′-CAGCCTTTAAGATAGGCTTGTCA-3′, UPL probe 5); *Ifnb1* (Ifnb1_for, 5′-CTGGCTTCCATCATGAACAA-3′; Ifnb1_rev, 5′-AGAGGGCTGTGGTGGAGAA-3′, UPL probe 18); *Ifit3* (Ifit3_for, 5′-TGGACTGAGATTTCTGAACTGC-3′; Ifit3_rev, 5′-AGAGATTCCCGGTTGACCTC-3′, UPL probe 3); *Cxcl10* (Cxcl10_for, 5′-GCTGCCGTCATTTTCTGC-3′; Cxcl10_rev, 5′-TCTCACTGGCCCGTCATC-3′, UPL probe 3). The levels of MCMV *IE1* and *E1* transcripts were determined as described previously (Stempel et al., 2019). Briefly, RNA was extracted from cells or spleen homogenates using the RNeasy Mini kit followed by DNase treatment as described above. Quantitative RT-PCR was performed using the OneStep RT-PCR Kit (Qiagen #210212) on a LightCycler 96 instrument (Roche). Absolute quantification of viral transcript numbers was performed using a dilution series of specific *in vitro* transcripts as standards. For normalisation, cellular β-actin transcripts were quantified in parallel. PCR primers and probe [5′ 6-FAM labelled and 3′ black hole quencher (BHQ) labelled] sequences were as follows: β-actin: β-actin_for, 5′-GACGGCCAGGTCATCACTATTG-3′, β-actin_rev, 5′-CACAGGATTCCATACCCAAGAAGG-3′, β-actin_probe, 5′-AACGAGCGGTTCCGATGCCC-3′; MCMV *IE1*: IE1_for, 5′-TGGCTGATTGATAGTTCTGTTTTATCA-3′, IE1_rev, 5′-CTCATGGACCGCATCGCT-3′, IE1_probe, 5′-AACGCTCCTCACTGCAGCATGCTTG-3′; MCMV *E1*: E1_for, 5′-TGCTCCCACTGAGGAAGAGAAGA-3′, E1_rev, 5′-GAGGCCGCTGCTGTAAC-AAT-3′, E1_probe, 5′-AGCCCAAGCGCCAGAAGACCCA-3′.

Statistical analysis

Differences between two data sets were evaluated by two-tailed unpaired Student's *t*-tests, in the case of viral transcript levels after log transformation of the data sets, using Graphpad Prism version 5.0 (GraphPad Software, San Diego, CA). $P<0.05$ was considered statistically significant.

Acknowledgements

We thank Christine Standfuß-Gabisch and Georg Wolf for excellent technical assistance.

Competing interests

The authors declare no competing or financial interests.

Author contributions

Conceptualization: M.M.B.; Methodology: E.R., M.S., B.C.; Validation: E.R., M.S., B.C.; Formal analysis: E.R., M.S., B.C.; Investigation: E.R., M.S., B.C.; Resources: M.M.B.; Data curation: E.R., M.S., B.C., H.B.; Writing - original draft: E.R., M.S., B.C., M.M.B.; Writing - review & editing: E.R., M.S., B.C., M.M.B.; Supervision: E.R., M.M.B.; Project administration: M.M.B.; Funding acquisition: M.M.B.

Funding
This study was funded by the Deutsche Forschungsgemeinschaft (DFG), BR3432/3-1. This work has been carried out within the framework of the SMART BIOTECS alliance between the Technische Universität Braunschweig and the Leibniz Universität Hannover, supported by the Ministry of Science and Culture (MWK) of Lower Saxony, Germany.

Supplementary information
Supplementary information available online at
http://jcs.biologists.org/lookup/doi/10.1242/jcs.246421.supplemental

Peer review history
The peer review history is available online at
https://jcs.biologists.org/lookup/doi/10.1242/jcs.246421.reviewer-comments.pdf

References

Abdelsalam, S. S., Korashy, H. M., Zeidan, A. and Agouni, A. (2019). The role of Protein Tyrosine Phosphatase (PTP)-1B in cardiovascular disease and its interplay with insulin resistance. *Biomolecules* **9**, 286. doi:10.3390/biom9070286

Anderie, I., Schulz, I. and Schmid, A. (2007). Direct interaction between ER membrane-bound PTP1B and its plasma membrane-anchored targets. *Cell. Signal.* **19**, 582-592. doi:10.1016/j.cellsig.2006.08.007

Blanchetot, C., Chagnon, M., Dube, N., Halle, M. and Tremblay, M. L. (2005). Substrate-trapping techniques in the identification of cellular PTP targets. *Methods* **35**, 44-53. doi:10.1016/j.ymeth.2004.07.007

Brinkmann, M. M., Spooner, E., Hoebe, K., Beutler, B., Ploegh, H. L. and Kim, Y.-M. (2007). The interaction between the ER membrane protein UNC93B and TLR3, 7, and 9 is crucial for TLR signaling. *J. Cell Biol.* **177**, 265-275. doi:10.1083/jcb.200612056

Bussey, K. A., Reimer, E., Todt, H., Denker, B., Gallo, A., Konrad, A., Ottinger, M., Adler, H., Sturzl, M., Brune, W. et al. (2014). The gammaherpesviruses Kaposi's sarcoma-associated herpesvirus and murine gammaherpesvirus 68 modulate the Toll-like receptor-induced proinflammatory cytokine response. *J. Virol.* **88**, 9245-9259. doi:10.1128/JVI.00841-14

Bussey, K. A., Murthy, S., Reimer, E., Chan, B., Hatesuer, B., Schughart, K., Glaunsinger, B., Adler, H. and Brinkmann, M. M. (2019). Endosomal toll-like receptors 7 and 9 cooperate in detection of murine Gammaherpesvirus 68 infection. *J. Virol.* **93**, e01173-e01118. doi:10.1128/JVI.01173-18

Carbone, C. J., Zheng, H., Bhattacharya, S., Lewis, J. R., Reiter, A. M., Henthorn, P., Zhang, Z.-Y., Baker, D. P., Ukkiramapandian, R., Bence, K. K. et al. (2012). Protein tyrosine phosphatase 1B is a key regulator of IFNAR1 endocytosis and a target for antiviral therapies. *Proc. Natl. Acad. Sci. USA* **109**, 19226-19231. doi:10.1073/pnas.1211491109

Carmichael, J. C., Yokota, H., Craven, R. C., Schmitt, A. and Wills, J. W. (2018). The HSV-1 mechanisms of cell-to-cell spread and fusion are critically dependent on host PTP1B. *PLoS Pathog.* **14**, e1007054. doi:10.1371/journal.ppat.1007054

Chan, B., Gonçalves Magalhães, V., Lemmermann, N. A. W., Juranić Lisnić, V., Stempel, M., Bussey, K. A., Reimer, E., Podlech, J., Lienenklaus, S., Reddehase, M. J. et al. (2017). The murine cytomegalovirus M35 protein antagonizes type I IFN induction downstream of pattern recognition receptors by targeting NF-κB mediated transcription. *PLoS Pathog.* **13**, e1006382. doi:10.1371/journal.ppat.1006382

Chernoff, J. (1999). Protein tyrosine phosphatases as negative regulators of mitogenic signaling. *J. Cell. Physiol.* **180**, 173-181. doi:10.1002/(SICI)1097-4652(199908)180:2<173::AID-JCP5>3.0.CO;2-Y

Content, J. (2009). Mechanisms of induction and action of interferons. *Verh. K Acad. Geneeskd. Belg.* **71**, 51-71.

Eden, E. R., White, I. J., Tsapara, A. and Futter, C. E. (2010). Membrane contacts between endosomes and ER provide sites for PTP1B-epidermal growth factor receptor interaction. *Nat. Cell Biol.* **12**, 267-272. doi:10.1038/ncb2026

Eisenberg-Bord, M., Shai, N., Schuldiner, M. and Bohnert, M. (2016). A tether is a tether is a tether: tethering at membrane contact sites. *Dev. Cell* **39**, 395-409. doi:10.1016/j.devcel.2016.10.022

Elchebly, M., Payette, P., Michaliszyn, E., Cromlish, W., Collins, S., Loy, A. L., Normandin, D., Cheng, A., Himms-Hagen, J., Chan, C.-C. et al. (1999). Increased insulin sensitivity and obesity resistance in mice lacking the protein tyrosine phosphatase-1B gene. *Science* **283**, 1544-1548. doi:10.1126/science.283.5407.1544

Feldhammer, M., Uetani, N., Miranda-Saavedra, D. and Tremblay, M. L. (2013). PTP1B: a simple enzyme for a complex world. *Crit. Rev. Biochem. Mol. Biol.* **48**, 430-445. doi:10.3109/10409238.2013.819830

Flint, A. J., Tiganis, T., Barford, D. and Tonks, N. K. (1997). Development of "substrate-trapping" mutants to identify physiological substrates of protein tyrosine phosphatases. *Proc. Natl. Acad. Sci. USA* **94**, 1680-1685. doi:10.1073/pnas.94.5.1680

Frangioni, J. V., Beahm, P. H., Shifrin, V., Jost, C. A. and Neel, B. G. (1992). The nontransmembrane tyrosine phosphatase PTP-1B localizes to the endoplasmic reticulum via its 35 amino acid C-terminal sequence. *Cell* **68**, 545-560. doi:10.1016/0092-8674(92)90190-N

Goldstein, B. J., Bittner-Kowalczyk, A., White, M. F. and Harbeck, M. (2000). Tyrosine dephosphorylation and deactivation of insulin receptor substrate-1 by protein-tyrosine phosphatase 1B. Possible facilitation by the formation of a ternary complex with the Grb2 adaptor protein. *J. Biol. Chem.* **275**, 4283-4289. doi:10.1074/jbc.275.6.4283

Goubau, D., Deddouche, S. and Reis e Sousa, C. (2013). Cytosolic sensing of viruses. *Immunity* **38**, 855-869. doi:10.1016/j.immuni.2013.05.007

Guo, Y., Li, D., Zhang, S., Yang, Y., Liu, J.-J., Wang, X., Liu, C., Milkie, D. E., Moore, R. P., Tulu, U. S. et al. (2018). Visualizing intracellular organelle and cytoskeletal interactions at nanoscale resolution on millisecond timescales. *Cell* **175**, 1430-1442.e17. doi:10.1016/j.cell.2018.09.057

Hemmi, H., Takeuchi, O., Kawai, T., Kaisho, T., Sato, S., Sanjo, H., Matsumoto, M., Hoshino, K., Wagner, H., Takeda, K. et al. (2000). A Toll-like receptor recognizes bacterial DNA. *Nature* **408**, 740-745. doi:10.1038/35047123

Hughes, S. K., Oudin, M. J., Tadros, J., Neil, J., del Rosario, A., Joughin, B. A., Ritsma, L., Wyckoff, J., Vasile, E., Eddy, R. et al. (2015). PTP1B-dependent regulation of receptor tyrosine kinase signaling by the actin-binding protein Mena. *Mol. Biol. Cell* **26**, 3867-3878. doi:10.1091/mbc.E15-06-0442

Isaacs, A. and Lindenmann, J. (1957). Virus interference. I. The interferon. *Proc. R. Soc. Lond. B Biol. Sci.* **147**, 258-267. doi:10.1098/rspb.1957.0048

Iwasaki, A. (2012). A virological view of innate immune recognition. *Annu. Rev. Microbiol.* **66**, 177-196. doi:10.1146/annurev-micro-092611-150203

Jia, Z., Barford, D., Flint, A. J. and Tonks, N. K. (1995). Structural basis for phosphotyrosine peptide recognition by protein tyrosine phosphatase 1B. *Science* **268**, 1754-1758. doi:10.1126/science.7540771

Jin, L., Hill, K. K., Filak, H., Mogan, J., Knowles, H., Zhang, B., Perraud, A.-L., Cambier, J. C. and Lenz, L. L. (2011). MPYS is required for IFN response factor 3 activation and type I IFN production in the response of cultured phagocytes to bacterial second messengers cyclic-di-AMP and cyclic-di-GMP. *J. Immunol.* **187**, 2595-2601. doi:10.4049/jimmunol.1100088

Jordan, S., Krause, J., Prager, A., Mitrovic, M., Jonjic, S., Koszinowski, U. H. and Adler, B. (2011). Virus progeny of murine cytomegalovirus bacterial artificial chromosome pSM3fr show reduced growth in salivary Glands due to a fixed mutation of MCK-2. *J. Virol.* **85**, 10346-10353. doi:10.1128/JVI.00545-11

Kaszubska, W., Falls, H. D., Schaefer, V. G., Haasch, D., Frost, L., Hessler, P., Kroeger, P. E., White, D. W., Jirousek, M. R. and Trevillyan, J. M. (2002). Protein tyrosine phosphatase 1B negatively regulates leptin signaling in a hypothalamic cell line. *Mol. Cell. Endocrinol.* **195**, 109-118. doi:10.1016/S0303-7207(02)00178-8

Klaman, L. D., Boss, O., Peroni, O. D., Kim, J. K., Martino, J. L., Zabolotny, J. M., Moghal, N., Lubkin, M., Kim, Y.-B., Sharpe, A. H. et al. (2000). Increased energy expenditure, decreased adiposity, and tissue-specific insulin sensitivity in protein-tyrosine phosphatase 1B-deficient mice. *Mol. Cell. Biol.* **20**, 5479-5489. doi:10.1128/MCB.20.15.5479-5489.2000

Lacy, P. and Stow, J. L. (2011). Cytokine release from innate immune cells: association with diverse membrane trafficking pathways. *Blood* **118**, 9-18. doi:10.1182/blood-2010-08-265892

Lienenklaus, S., Cornitescu, M., Zietara, N., Łyszkiewicz, M., Gekara, N., Jabłońska, J., Edenhofer, F., Rajewsky, K., Bruder, D., Hafner, M. et al. (2009). Novel reporter mouse reveals constitutive and inflammatory expression of IFN-β in vivo. *J. Immunol.* **183**, 3229-3236. doi:10.4049/jimmunol.0804277

Lio, C.-W. J., McDonald, B., Takahashi, M., Dhanwani, R., Sharma, N., Huang, J., Pham, E., Benedict, C. A. and Sharma, S. (2016). cGAS-STING signaling regulates initial innate control of cytomegalovirus infection. *J. Virol.* **90**, 7789-7797. doi:10.1128/JVI.01040-16

Low, P. C., Misaki, R., Schroder, K., Stanley, A. C., Sweet, M. J., Teasdale, R. D., Vanhaesebroeck, B., Meunier, F. A., Taguchi, T. and Stow, J. L. (2010). Phosphoinositide 3-kinase δ regulates membrane fission of Golgi carriers for selective cytokine secretion. *J. Cell Biol.* **190**, 1053-1065. doi:10.1083/jcb.201001028

Lu, X., Malumbres, R., Shields, B., Jiang, X., Sarosiek, K. A., Natkunam, Y., Tiganis, T. and Lossos, I. S. (2008). PTP1B is a negative regulator of interleukin 4-induced STAT6 signaling. *Blood* **112**, 4098-4108. doi:10.1182/blood-2008-03-148726

Manderson, A. P., Kay, J. G., Hammond, L. A., Brown, D. L. and Stow, J. L. (2007). Subcompartments of the macrophage recycling endosome direct the differential secretion of IL-6 and TNFα. *J. Cell Biol.* **178**, 57-69. doi:10.1083/jcb.200612131

Mathys, S., Schroeder, T., Ellwart, J., Koszinowski, U. H., Messerle, M. and Just, U. (2003). Dendritic cells under influence of mouse cytomegalovirus have a physiologic dual role: to initiate and to restrict T cell activation. *J. Infect. Dis.* **187**, 988-999. doi:10.1086/368094

Michallet, M.-C., Meylan, E., Ermolaeva, M. A., Vazquez, J., Rebsamen, M., Curran, J., Poeck, H., Bscheider, M., Hartmann, G., König, M. et al. (2008). TRADD protein is an essential component of the RIG-like helicase antiviral pathway. *Immunity* **28**, 651-661. doi:10.1016/j.immuni.2008.03.013

Mogensen, T. H. (2009). Pathogen recognition and inflammatory signaling in innate immune defenses. *Clin. Microbiol. Rev.* **22**, 240-273, Table of Contents. doi:10.1128/CMR.00046-08

Murray, R. Z. and Stow, J. L. (2014). Cytokine secretion in macrophages: SNAREs, Rabs, and membrane trafficking. *Front. Immunol.* **5**, 538. doi:10.3389/fimmu.2014.00538

Murray, R. Z., Kay, J. G., Sangermani, D. G. and Stow, J. L. (2005a). A role for the phagosome in cytokine secretion. *Science* **310**, 1492-1495. doi:10.1126/science.1120225

Murray, R. Z., Wylie, F. G., Khromykh, T., Hume, D. A. and Stow, J. L. (2005b). Syntaxin 6 and Vti1b form a novel SNARE complex, which is up-regulated in activated macrophages to facilitate exocytosis of tumor necrosis Factor-α. *J. Biol. Chem.* **280**, 10478-10483. doi:10.1074/jbc.M414420200

Myers, M. P., Andersen, J. N., Cheng, A., Tremblay, M. L., Horvath, C. M., Parisien, J.-P., Salmeen, A., Barford, D. and Tonks, N. K. (2001). TYK2 and JAK2 are substrates of protein-tyrosine phosphatase 1B. *J. Biol. Chem.* **276**, 47771-47774. doi:10.1074/jbc.C100583200

Nixon-Abell, J., Obara, C. J., Weigel, A. V., Li, D., Legant, W. R., Xu, C. S., Pasolli, H. A., Harvey, K., Hess, H. F., Betzig, E. et al. (2016). Increased spatiotemporal resolution reveals highly dynamic dense tubular matrices in the peripheral ER. *Science* **354**, aaf3928. doi:10.1126/science.aaf3928

Ozek, C., Kanoski, S. E., Zhang, Z.-Y., Grill, H. J. and Bence, K. K. (2014). Protein-tyrosine phosphatase 1B (PTP1B) is a novel regulator of central brain-derived neurotrophic factor and tropomyosin receptor kinase B (TrkB) signaling. *J. Biol. Chem.* **289**, 31682-31692. doi:10.1074/jbc.M114.603621

Paludan, S. R. and Bowie, A. G. (2013). Immune sensing of DNA. *Immunity* **38**, 870-880. doi:10.1016/j.immuni.2013.05.004

Pestka, S. (2007). The interferons: 50 years after their discovery, there is much more to learn. *J. Biol. Chem.* **282**, 20047-20051. doi:10.1074/jbc.R700004200

Sangwan, V., Abella, J., Lai, A., Bertos, N., Stuible, M., Tremblay, M. L. and Park, M. (2011). Protein-tyrosine phosphatase 1B modulates early endosome fusion and trafficking of Met and epidermal growth factor receptors. *J. Biol. Chem.* **286**, 45000-45013. doi:10.1074/jbc.M111.270934

Scorrano, L., de Matteis, M. A., Emr, S., Giordano, F., Hajnóczky, G., Kornmann, B., Lackner, L. L., Levine, T. P., Pellegrini, L., Reinisch, K. et al. (2019). Coming together to define membrane contact sites. *Nat. Commun.* **10**, 1287. doi:10.1038/s41467-019-09253-3

Seely, B. L., Staubs, P. A., Reichart, D. R., Berhanu, P., Milarski, K. L., Saltiel, A. R., Kusari, J. and Olefsky, J. M. (1996). Protein tyrosine phosphatase 1B interacts with the activated insulin receptor. *Diabetes* **45**, 1379-1385. doi:10.2337/diab.45.10.1379

Solodova, E., Jablonska, J., Weiss, S. and Lienenklaus, S. (2011). Production of IFN-β during Listeria monocytogenes infection is restricted to monocyte/macrophage lineage. *PLoS One* **6**, e18543. doi:10.1371/journal.pone.0018543

Stark, G. R. and Darnell, J. E. Jr. (2012). The JAK-STAT pathway at twenty. *Immunity* **36**, 503-514. doi:10.1016/j.immuni.2012.03.013

Stark, G. R., Kerr, I. M., Williams, B. R. G., Silverman, R. H. and Schreiber, R. D. (1998). How cells respond to interferons. *Annu. Rev. Biochem.* **67**, 227-264. doi:10.1146/annurev.biochem.67.1.227

Stempel, M., Chan, B., Juranić Lisnić, V., Krmpotić, A., Hartung, J., Paludan, S. R., Füllbrunn, N., Lemmermann, N. A. W. and Brinkmann, M. M. (2019). The herpesviral antagonist m152 reveals differential activation of STING-dependent IRF and NF-kappaB signaling and STING's dual role during MCMV infection. *EMBO J.* **38**, e100983. doi:10.15252/embj.2018100983

Stow, J. L., Manderson, A. P. and Murray, R. Z. (2006). SNAREing immunity: the role of SNAREs in the immune system. *Nat. Rev. Immunol.* **6**, 919-929. doi:10.1038/nri1980

Stuible, M. and Tremblay, M. L. (2010). In control at the ER: PTP1B and the down-regulation of RTKs by dephosphorylation and endocytosis. *Trends Cell Biol.* **20**, 672-679. doi:10.1016/j.tcb.2010.08.013

Stuible, M., Abella, J. V., Feldhammer, M., Nossov, M., Sangwan, V., Blagoev, B., Park, M. and Tremblay, M. L. (2010). PTP1B targets the endosomal sorting machinery: dephosphorylation of regulatory sites on the endosomal sorting complex required for transport component STAM2. *J. Biol. Chem.* **285**, 23899-23907. doi:10.1074/jbc.M110.115295

Tabeta, K., Georgel, P., Janssen, E., Du, X., Hoebe, K., Crozat, K., Mudd, S., Shamel, L., Sovath, S., Goode, J. et al. (2004). Toll-like receptors 9 and 3 as essential components of innate immune defense against mouse cytomegalovirus infection. *Proc. Natl. Acad. Sci. USA* **101**, 3516-3521. doi:10.1073/pnas.0400525101

Tabeta, K., Hoebe, K., Janssen, E. M., Du, X., Georgel, P., Crozat, K., Mudd, S., Mann, N., Sovath, S., Goode, J. et al. (2006). The Unc93b1 mutation 3d disrupts exogenous antigen presentation and signaling via Toll-like receptors 3, 7 and 9. *Nat. Immunol.* **7**, 156-164. doi:10.1038/ni1297

Tonks, N. K. (2013). Special issue: protein phosphatases: from molecules to networks: introduction. *FEBS J.* **280**, 323. doi:10.1111/febs.12098

Través, P. G., Pardo, V., Pimentel-Santillana, M., González-Rodríguez, A., Mojena, M., Rico, D., Montenegro, Y., Calés, C., Martín-Sanz, P., Valverde, A. M. et al. (2014). Pivotal role of protein tyrosine phosphatase 1B (PTP1B) in the macrophage response to pro-inflammatory and anti-inflammatory challenge. *Cell Death Dis.* **5**, e1125. doi:10.1038/cddis.2014.90

Vieira, M. N., Lyra, E. S. N. M., Ferreira, S. T. and DE Felice, F. G. (2017). Protein Tyrosine Phosphatase 1B (PTP1B): a potential target for Alzheimer's therapy? *Front. Aging Neurosci.* **9**, 7. doi:10.3389/fnagi.2017.00007

Woodford-Thomas, T. A., Rhodes, J. D. and Dixon, J. E. (1992). Expression of a protein tyrosine phosphatase in normal and v-src-transformed mouse 3T3 fibroblasts. *J. Cell Biol.* **117**, 401-414. doi:10.1083/jcb.117.2.401

Wu, J. and Chen, Z. J. (2014). Innate immune sensing and signaling of cytosolic nucleic acids. *Annu. Rev. Immunol.* **32**, 461-488. doi:10.1146/annurev-immunol-032713-120156

Wu, H., Carvalho, P. and Voeltz, G. K. (2018). Here, there, and everywhere: the importance of ER membrane contact sites. *Science* **361**, eaan5835. doi:10.1126/science.aan5835

Xia, T., Yi, X.-M., Wu, X., Shang, J. and Shu, H.-B. (2019). PTPN1/2-mediated dephosphorylation of MITA/STING promotes its 20S proteasomal degradation and attenuates innate antiviral response. *Proc. Natl. Acad. Sci. USA* **116**, 20063-20069. doi:10.1073/pnas.1906431116

Xie, L., Zhang, Y.-L. and Zhang, Z.-Y. (2002). Design and characterization of an improved protein tyrosine phosphatase substrate-trapping mutant. *Biochemistry* **41**, 4032-4039. doi:10.1021/bi015904r

Xu, H., An, H., Hou, J., Han, C., Wang, P., Yu, Y. and Cao, X. (2008). Phosphatase PTP1B negatively regulates MyD88- and TRIF-dependent proinflammatory cytokine and type I interferon production in TLR-triggered macrophages. *Mol. Immunol.* **45**, 3545-3552. doi:10.1016/j.molimm.2008.05.006

Young, M. W. and Kim, Y. (2019). Dephosphorylation of epidermal growth factor receptor by protein tyrosine phosphatase 1B. *FASEB J.* **33**, 645.5-645.5.

Yue, L., Xie, Z., Li, H., Pang, Z., Junkins, R. D., Tremblay, M. L., Chen, X. and Lin, T.-J. (2016). Protein tyrosine phosphatase-1B negatively impacts host defense against pseudomonas aeruginosa infection. *Am. J. Pathol.* **186**, 1234-1244. doi:10.1016/j.ajpath.2016.01.005

Zabolotny, J. M., Bence-Hanulec, K. K., Stricker-Krongrad, A., Haj, F., Wang, Y., Minokoshi, Y., Kim, Y.-B., Elmquist, J. K., Tartaglia, L. A., Kahn, B. B. et al. (2002). PTP1B regulates leptin signal transduction in vivo. *Dev. Cell* **2**, 489-495. doi:10.1016/S1534-5807(02)00148-X

Zhang, S. and Zhang, Z. Y. (2007). PTP1B as a drug target: recent developments in PTP1B inhibitor discovery. *Drug Discov. Today* **12**, 373-381. doi:10.1016/j.drudis.2007.03.011

Zhang, J., Li, L., Li, J., Liu, Y., Zhang, C.-Y., Zhang, Y. and Zen, K. (2015). Protein tyrosine phosphatase 1B impairs diabetic wound healing through vascular endothelial growth factor receptor 2 dephosphorylation. *Arterioscler. Thromb. Vasc. Biol.* **35**, 163-174. doi:10.1161/ATVBAHA.114.304705